XLAB RESEARCH REPORT: STATUS OF ADAPTATION TO CLIMATE RISK IN PAKISTAN

ABSTRACT: Global warming due to anthropogenic climate change is thought to be responsible for, among its numerous other effects, an increase in the frequency and strength of floods and drought-like conditions in Pakistan. At the same time, Pakistan is also experiencing steady population growth (currently 240 million and increasing at approximately 2% every year) and, reportedly, haphazard, climate-unadaptive urbanization, often through the conversion of agricultural lands to urban housing societies. This research aims to derive general trends in land use conversion, population growth and climatic conditions in Pakistan's Lahore district from remote sensing data to inform climate-adaptive development policymaking in Pakistan.

I.Theory, Background and Process

Climate Change in Pakistan

Extreme precipitation during the monsoon season (July to August) is considered to have caused the 2010 and 2022 floods in Pakistan (Nanditha, J. S., et al, 2023), where each event resulted in the displacement of more than 30 million persons, and billions of dollars in economic damages (Reuters, 2022)(Scale of Pakistan's flooding, 2022). At the peak of the flood, tens of thousands of square kilometers of area remain submerged in both 2022 and 2010 (Devastating Floods in Pakistan). In addition to riverine and precipitation induced floods, heat waves, drought (exacerbated by degradation of the Indus Basin, which houses the bulk of Pakistan's population and economy (Yu et. al, 2013), and glacial lake outburst floods are also intensifying due to climate change (Chaudhry, 2017).

With more than 240 million people, Pakistan is the fifth most populous country in the world and growing at approximately 2% per year (World Bank Open Data). Haphazard, climate-unadaptive urbanization, often through the conversion of agricultural lands to urban housing societies has been increasingly reported in various regions in Pakistan (Arslan, 2022) and poses a danger to resilience to changing trends in climate.

Many risk indices attempt to quantify on a scale the expected impact of climate change on growth in a country. According to the INFORM Climate Change Risk Index, Pakistan has a Baseline CC risk index of 6.0 out of 10 (high risk) in 2022. In an optimistic scenario, it is projected to have a CC risk index of 7.8 in 2050 and 7.7 in 2080. In a pessimistic scenario, it is projected to have a CC risk index of 7.9 in 2050 and 8.1 in 2080. In both scenarios, Pakistan is classified as being at high risk from Climate Change.

Risk Indices and Relevant Concepts/Definitions:

In recent years, risk due to climate change, natural disasters and other causes has been increasingly described by international development organizations and scientific bodies in the form of values on risk indices. These indices, which use a common vocabulary and definitions of terms like risk or resilience, are developed as variants of the following formula: risk as a function of exposure to natural disaster and the capacity to cope with such exposure. Each index calculates these scores differently, with different weights assigned to the formula components and different datasets and statistics being used to quantify each component. Some commonly used risk indices are described below:

The INFORM Climate Change Risk Index: incorporates climate and socio-economic projections to show how risk will evolve in the medium to long term, and how climate will impact future crises. Climate projections are incorporated through Representative Concentration Pathways, which describe how the concentration of greenhouse gases and radiative forcings in the atmosphere will change over time. These are RCP2.6, a stringent mitigation scenario, RCP4.5 and RCP6.0, two intermediate scenarios and RCP8.5, a high emissions scenario. Similarly, different socio-economic pathways can be used to calculate evolution of future risk. The SSP1 represents an optimistic socio-economic scenario where global population peaks around 2050, development is high paced and sustainable, technological innovation is based on low carbon energy sources and land is highly productive. The SSP3 on the other hand envisages low-income growth and human capital investments, high population growth rates in low-income countries, and low migration and urbanization. The Inform Climate Change Risk Index calculates country-wise risk indices in an optimistic scenario that combines RCP 4.5 and SSP1, and in a pessimistic scenario that combines RCP8.5 and SSP3.

Global Climate Risk Index: focuses on extreme weather (not climate) events (storms, floods, heatwaves) but not slow onset processes like rising sea levels, glacier melting, ocean warming, acidification. It is based on past data and analysis from MunichRe's NatCatSERVICE, which documents the extent and intensity of individual natural hazard events worldwide, number of total losses caused, number of deaths, insured damages and total economic damages. The indicators used to build the CRI are: a. number of deaths b. number of deaths per 100,000 inhabitants (sourced from the IMF) c. sum of losses in PPP (IMF) d. losses per unit of GDP (IMF). The index score is calculated by assigning the following weights: death toll (1/6), deaths per 100,000 inhabitants (1/3), absolute losses in PPP (1/6), losses per GDP unit (1/3).

World Risk Index: is calculated by taking exposure to mean physical exposure, which refers to the potential average annual number of individuals who are exposed to floods, droughts etc.

Notre Dame Global Adaptation Initiative Country Index: is composed of two key dimensions of adaptation: vulnerability and readiness. Vulnerability measures a country's exposure, sensitivity and capacity to adapt to the negative effects of climate change. Six sectors are used to measure overall vulnerability: food, water, health, ecosystem service, human habitat and infrastructure. Exposure here is the degree to which a system is exposed to significant climate change from a biophysical perspective. It is a component of vulnerability independent of socioeconomic context. Exposure indicators are projected impacts for the coming decades and are invariant over time in ND-GAIN (projected change of flood hazard, projected change of warm periods).

EU Global Climate Change Alliance plus Flagship Initiative index: relevant indicators to climate change used to calculate the index include the frequency of drought events, frequency of flood events, frequency of storm events, people exposed to drought events, people exposed to flood events, people exposed to storm events,and the number of internally displaced people.

The following definitions from the Global Assessment Report on Disaster Risk Reduction, 2022 help illustrate the scope of the constituents of risk as described above:

Disaster: "serious disruption of the functioning of a community or a society at any scale due to hazardous events interacting with conditions of exposure, vulnerability and capacity, leading to one or more of the following: human, material, economic and environmental losses and impacts. Disasters stem from a combination of hazards with vulnerability and exposure of people and assets."

Hazard: "a process, phenomenon or human activity that may cause loss of life, injury or other health impacts, property damage, social and economic disruption or environmental degradation."

Vulnerability: "the conditions determined by physical, social, economic and environmental factors or processes which increase the susceptibility of an individual, a community, assets or systems to the impacts of hazards". Exposure is the "situation of people, infrastructure, housing, production capacities and other tangible human assets located in hazard-prone areas. When hazards combine with vulnerability and exposure, disasters are most likely to occur because exposure increases the impacts and vulnerability reduces coping capacity."

Climate Modeling and projections

While some risk indices rely on the use of past data to calculate risk due to climate change, indices like the Inform Climate Change Risk Index rely on emissions and growth projections from climate models standardized by the United Nations' Intergovernmental Panel on Climate Change (Coupled Model Intercomparison Project) to predict future risk.

Climate models abide by fundamental principles of physics e.g. law of conservation of energy, the Stefan-Boltzmann Law (natural greenhouse effect), the Clausius-Clapeyron equation (relationship between air temperature and maximum water vapour pressure), the Navier-Stokes equations of fluid motion (capturing speed, pressure, temperature, density of gases in atmosphere and water in the ocean). The interactions of small scale processes in a model creates a simulation of climate. The code for climate models is typically written in Fortran, along with C for global models run on supercomputers. The Earth is divided up into a series of grid cells with several layers across the height of the atmosphere and depth of the ocean, calculating the state of the climate system in each cell. For processes that occur on scales smaller than the grid cell (e.g. convection), approximations are used. The size of the grid cells is the spatial resolution of the model. Time-step is how often the model calculates the state of the climate system. A time step of 30 minutes is currently considered a reasonable compromise between accuracy and computer processing time. Energy Balance Models and Global Climate Models (including Earth System Models) are combined to produce coupled climate models. Integrated Assessment Models add societal aspects such as population, economic growth and energy use to coupled climate models, producing future GHG emissions scenarios. Inputs into climate models include forcings (e.g. sun's output, GHGs CO2, CH4, N2O, aerosols (CMIP6 has approximately 16 petabytes of data). Control runs where radiative forcings are held constant for hundreds of years allow an assessment of human induced climate variability. Climate model outputs comprise thousands of variables in the Earth's climate: temperatures, humidity, ocean salinity and acidity, snow cover and glacier extent, jet stream, ocean currents.

In spite of the incredible complexity and volume of data input into climate models, questions about the utility of the models' outputs have been raised recently. In general, climate risk assessments tend to assess climate change primarily in terms of global mean temperature change, whereas GHG emissions affect other aspects of the global system including rainfall patterns, ocean acidity, extreme weather, energy balance between upper and lower atmosphere and oceans. Also since these assessments are unidirectional, they do not account for the impact of human response to climate change. Existing climate and integrated assessment models focus on the direct effects of climate change, while the greatest risks may arise from the indirect effects of climate change. Also local effects can differ significantly from the global average or even country level effects, which makes an inquiry into regional/local effects of climate change indispensable.

Research Question

The goal of the study is to superimpose climate change trends on the land conversion and population expansion trends in Pakistan to ascertain the gap in climate adaptive development. The variables of concern in this research are population expanse, impervious surface cover due to urbanization, floodplain extent, water balance using precipitation and evapotranspiration and rangeland cover. Mean land surface temperatures over a 15-year period have also been calculated to serve as an indicator for general warming trends. For greater visual clarity and analysis of local trends, the Lahore district, which is the second most populous district of Pakistan and is located in the Punjab province on the bank of River Ravi, is focused for each of the above variables. The 2022 flood in Pakistan is visualized using SAR imagery from August 2022 in Larkana, Sindh, and is compared with the SAR imagery of Lahore from the same period.

Visualization of Climate Change effects using Geospatial data

The following workflows are used to arrive at the results in this research, adapted from the book "Cloud Based Remote Sensing with Google Earth Engine: Fundamentals and Applications" (www.eefabook.org):

i. Estimating Population within a settlement (1990, 2000, 2015)

ii. Expansion of impervious surfaces in floodplain (from 2010 to 2018)

iii. Land Surface Temperature (2005-2010, 2010-2015, 2015-2020)

iv. Surface Water Mapping and Otsu's method to extract flooded areas (2022)

v. Time series precipitation and evapotranspiration and vegetation and drought indices. Monthly water balance, NDVI as vegetation index and MSI as drought index (2010 to 2020)

vi. Land cover change in rangeland (2001, 2009, 2016)

Datasets used:

i. Global Administrative Unit Layers Dataset 2015 (FAO, UN)

ii. WorldPop (www.worldpop.org; DOI: 10.5258/SOTON/WP00645)

iii. Global Human Settlement Layer (DOI: 10.2905/2FF68A52-5B5B-4A22-8F40-C41DA8332CFE)

iv. Global Artificial Impervious Area Dataset (DOI: https://doi.org/10.1007/s11430-020-9797-9)

v. Global Flood Database (DOI: doi:10.1038/s41586-021-03695-w)

vi. MYD11A2.061 Aqua Land Surface Temperature and Emissivity 8-Day Global 1km (https://doi.org/10.5067/MODIS/MYD11A2.061)

vii. Sentinel-1 SAR data 2022

viii. Global Surface Water Dataset (DOI: doi:10.1038/nature20584)

ix. CHIRPS: Climate Hazards Group Infrared Precipitation with Station Data (a quasi-global rainfall dataset spanning 35 years of precipitation records at a 5 km resolution compiled by combining data from meteorological stations and satellite data) (DOI: http://dx.doi.org/10.15780/G2WC70)

x. MOD16: Algorithm based on the Penman-Monteith equation which uses daily meteorological reanalysis data and remotely sensed vegetation property dynamics. It can be used for evapotranspiration estimation (DOI: https://doi.org/10.5067/MODIS/MOD16A2.061)

xi. MOD13: MODIS/Terra Vegetation Indices (https://doi.org/10.5067/MODIS/MOD13Q1.061)

xii. MOD09: MODIS/Terra Atmospherically Corrected Surface Reflectance (DOI: https://doi.org/10.5067/MODIS/MOD13Q1.061)

xiii. ESA WorldCover 2020 (https://doi.org/10.5281/zenodo.5571936)

xiv. MCD12Q1: MODIS/Terra + Aqua Land Cover Type Yearly (DOI: https://doi.org/10.5067/MODIS/MCD12Q1.061)

II. Results

A. POPULATION EXPANSE

- Population layer in 2000, Pakistan:

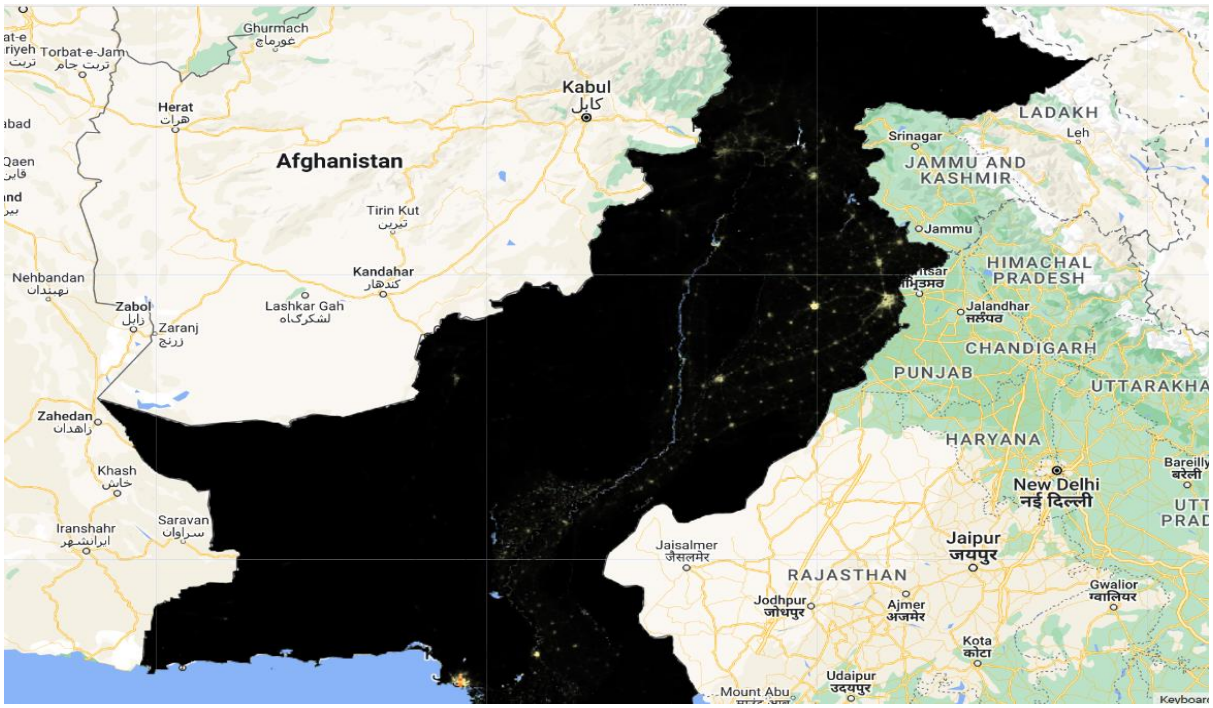

- Population layer in 2000, Lahore district:

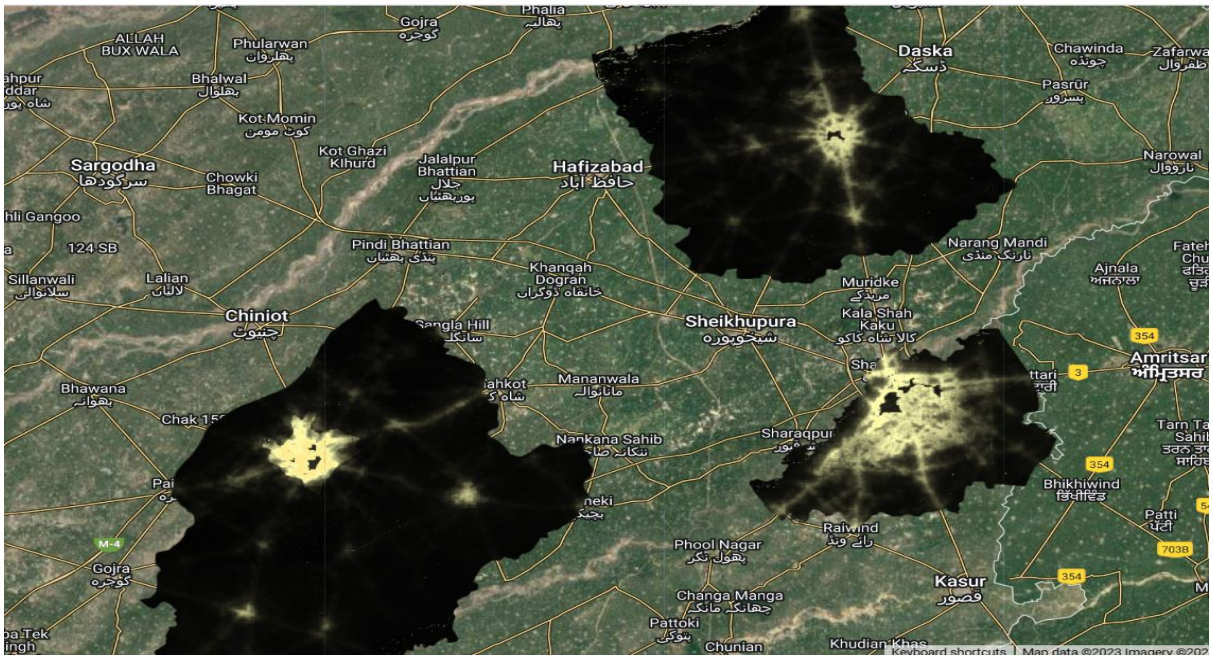

- Population layer in 2020, Pakistan:

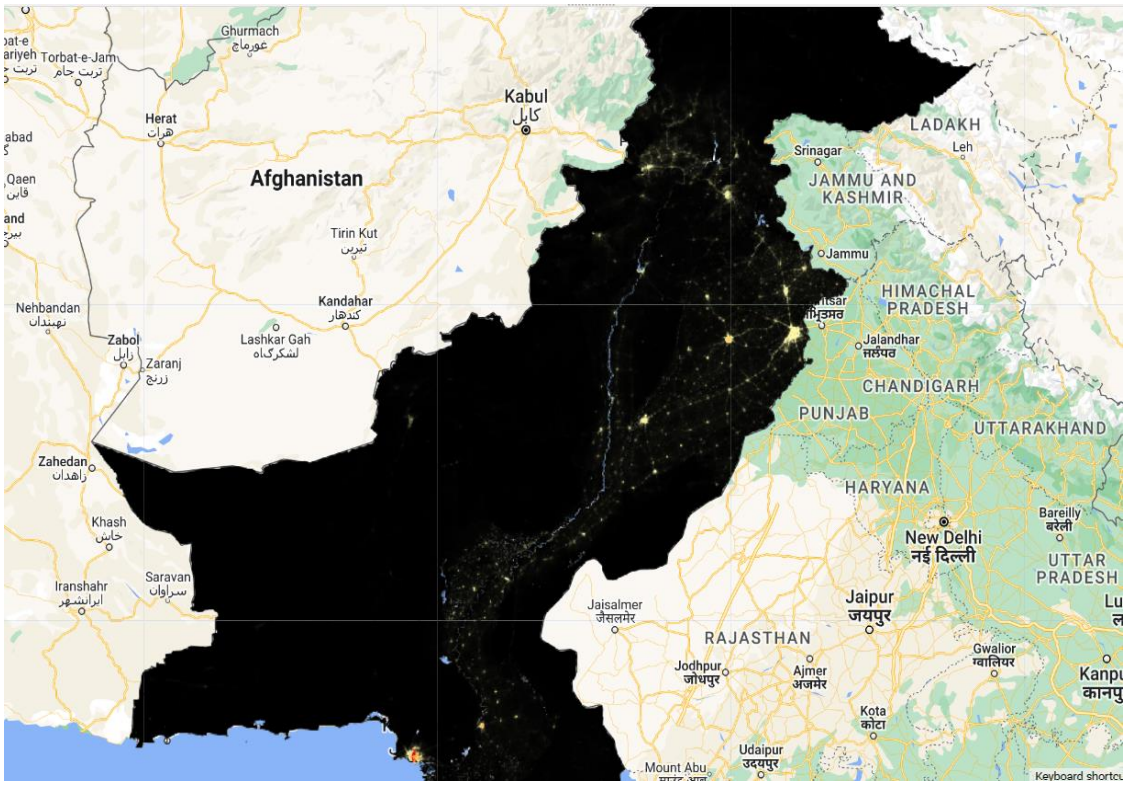

- Population layer in 2020, Lahore district:

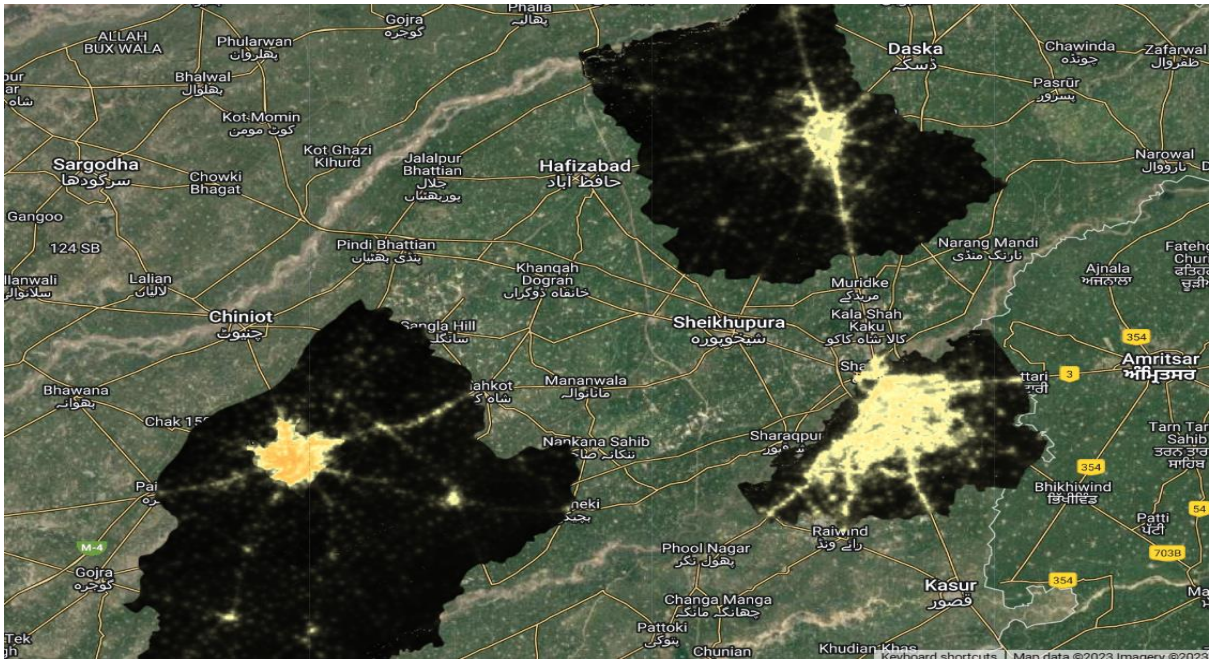

- Global Human Settlement Layer, Lahore 1990: Population estimate: 4,970,158
- (Pakistan population estimate 1990: 104,813,017)

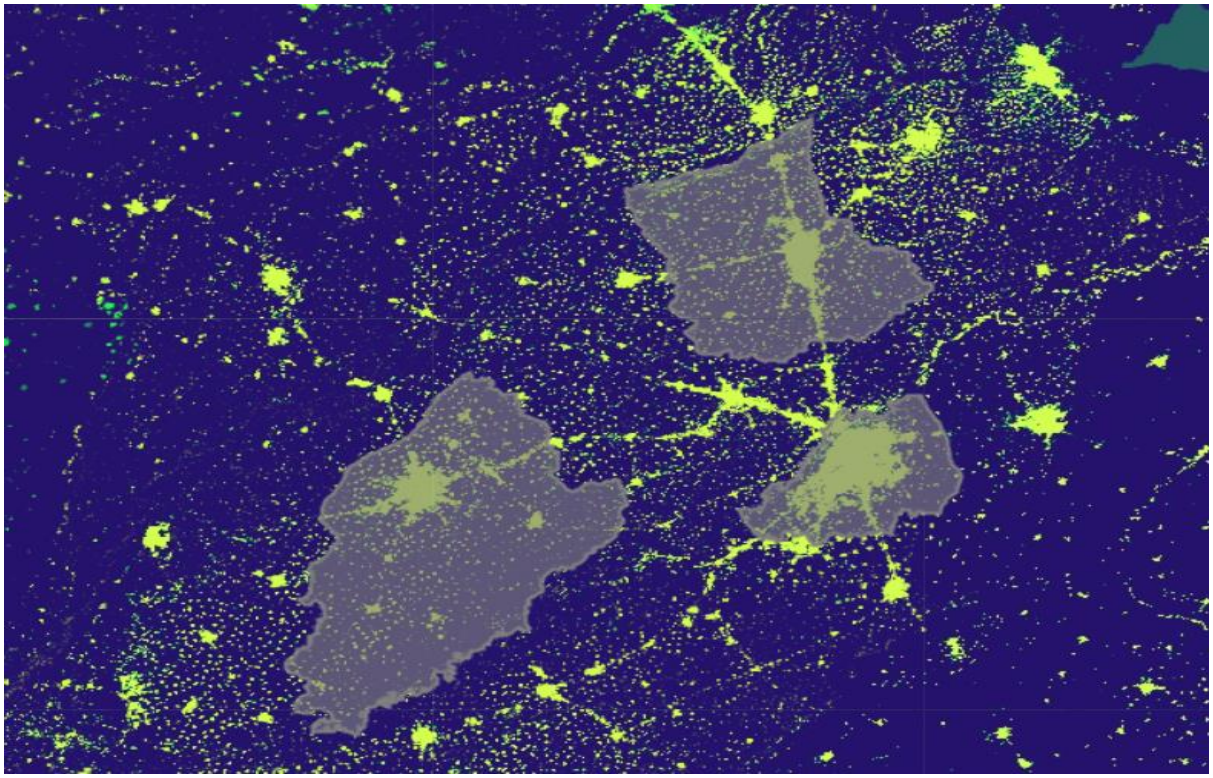

- Global Human Settlement Layer, Lahore 2000: Population estimate: 6,449,726
- (Pakistan population estimate 2000: 134,912,583)

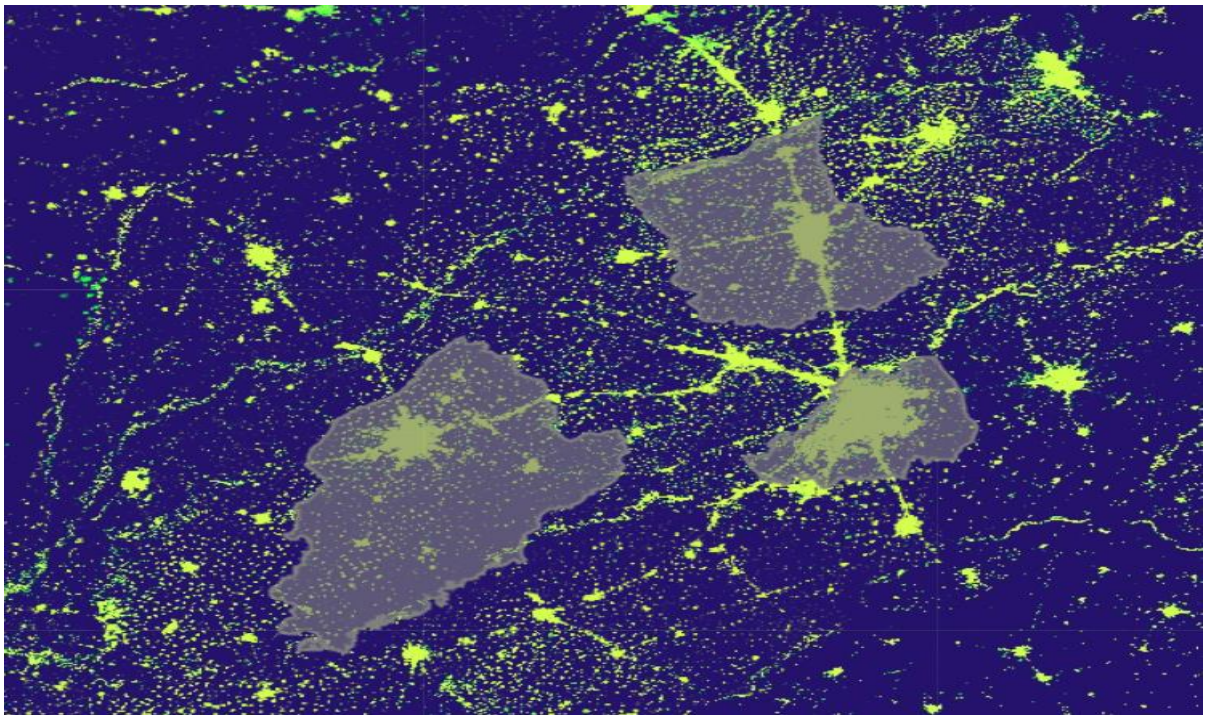

- Global Human Settlement Layer, Lahore 2015: Population estimate: 8,923,281
- (Pakistan population estimate 2015: 184,932,281)

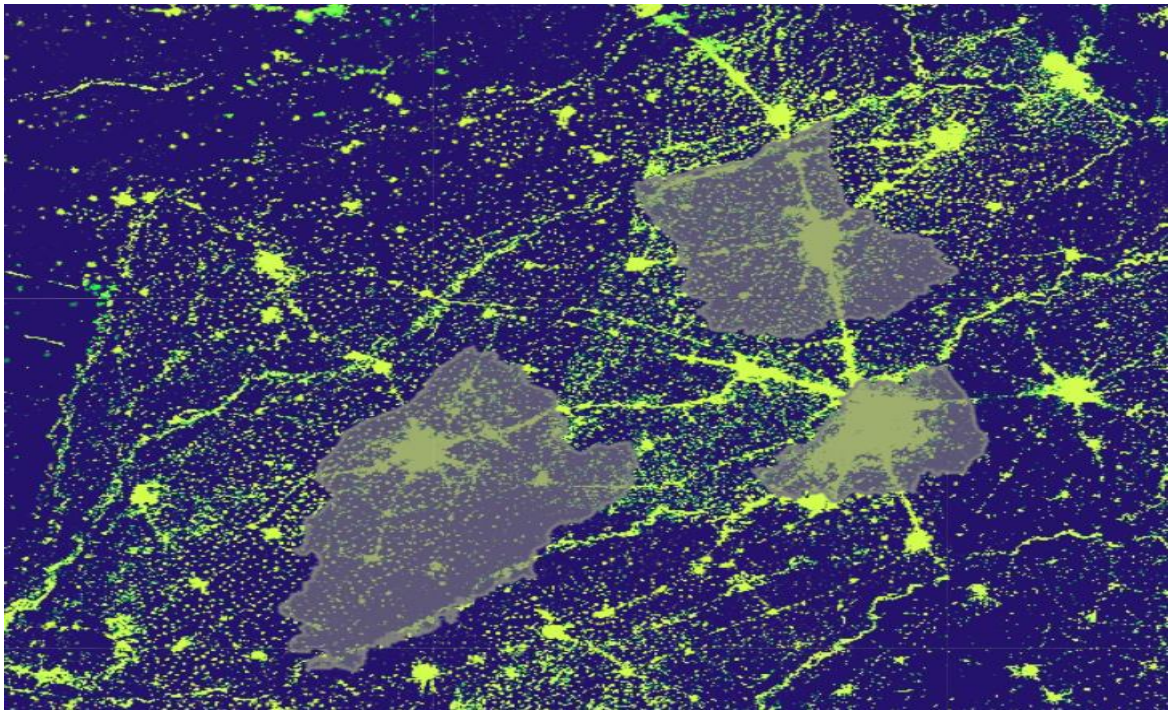

B. URBAN EXPANSION AND FLOODPLAIN

- GFD Satellite Observed Floodplain:

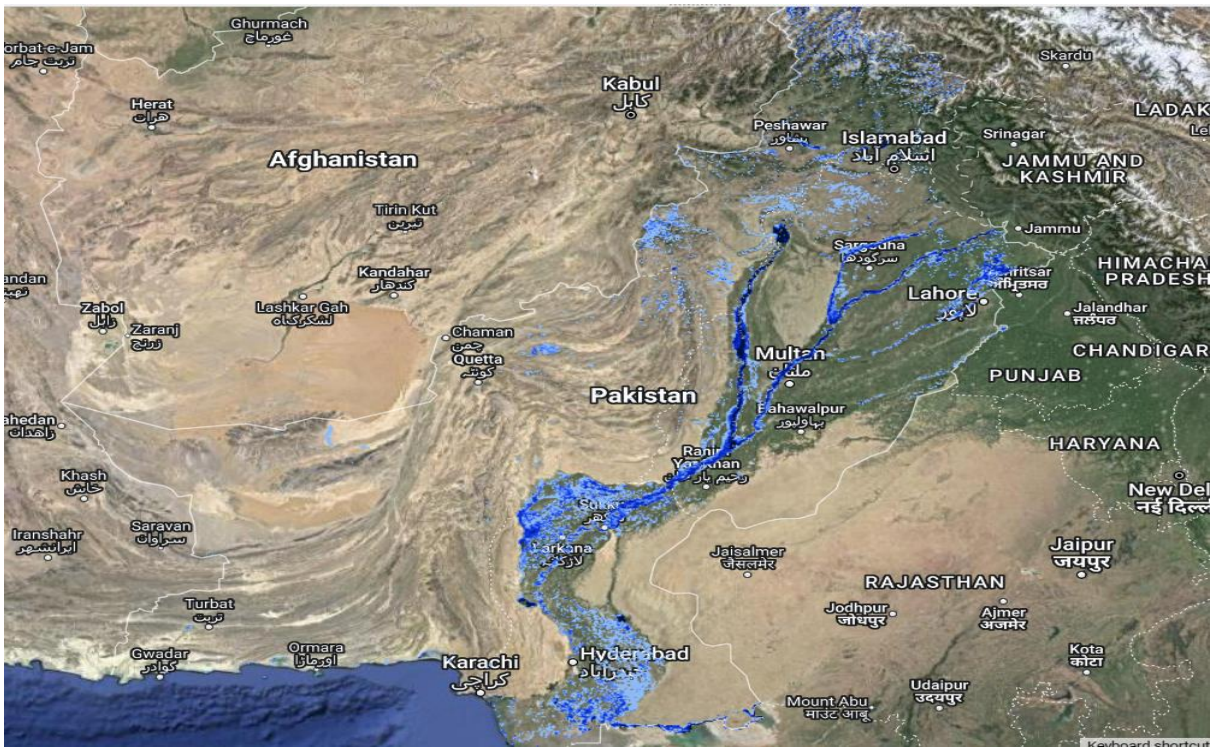

- GFD Satellite Observed Floodplain in Lahore district:

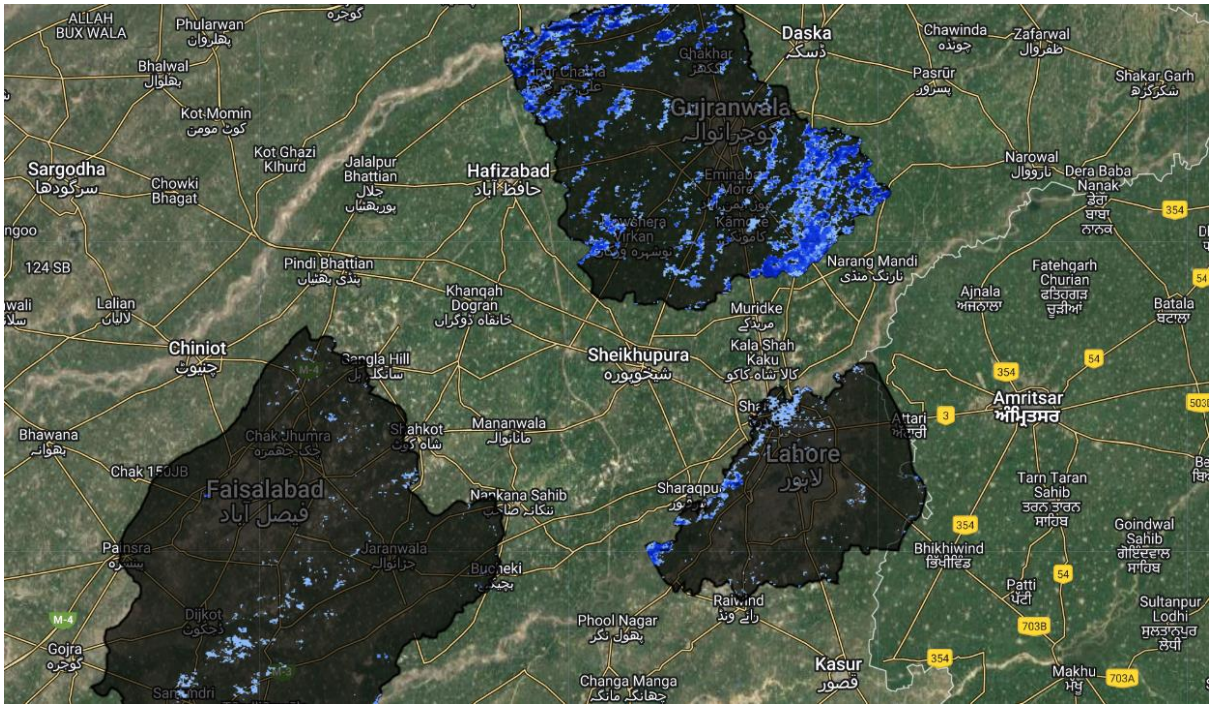

- Impervious Surfaces in 2000:

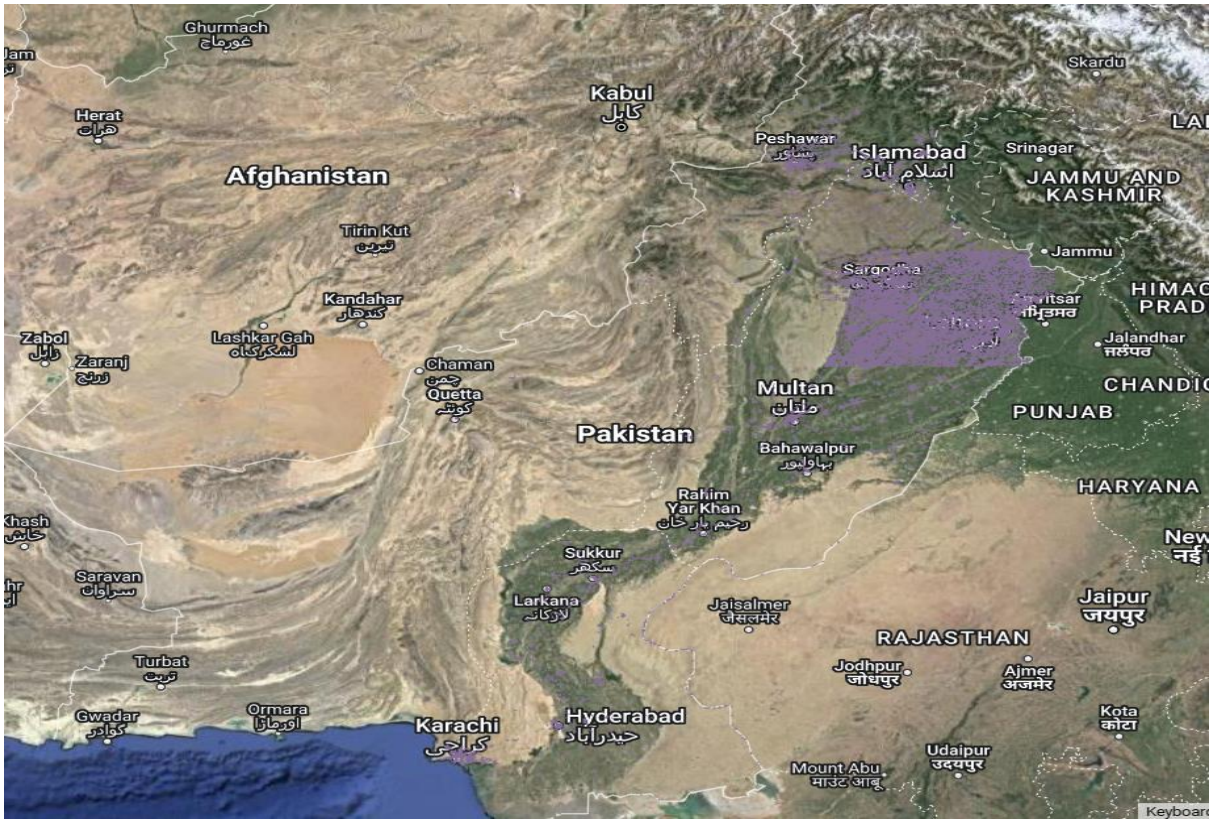

- Impervious Surfaces in 2018:

- Impervious surfaces in Lahore district in 2018:

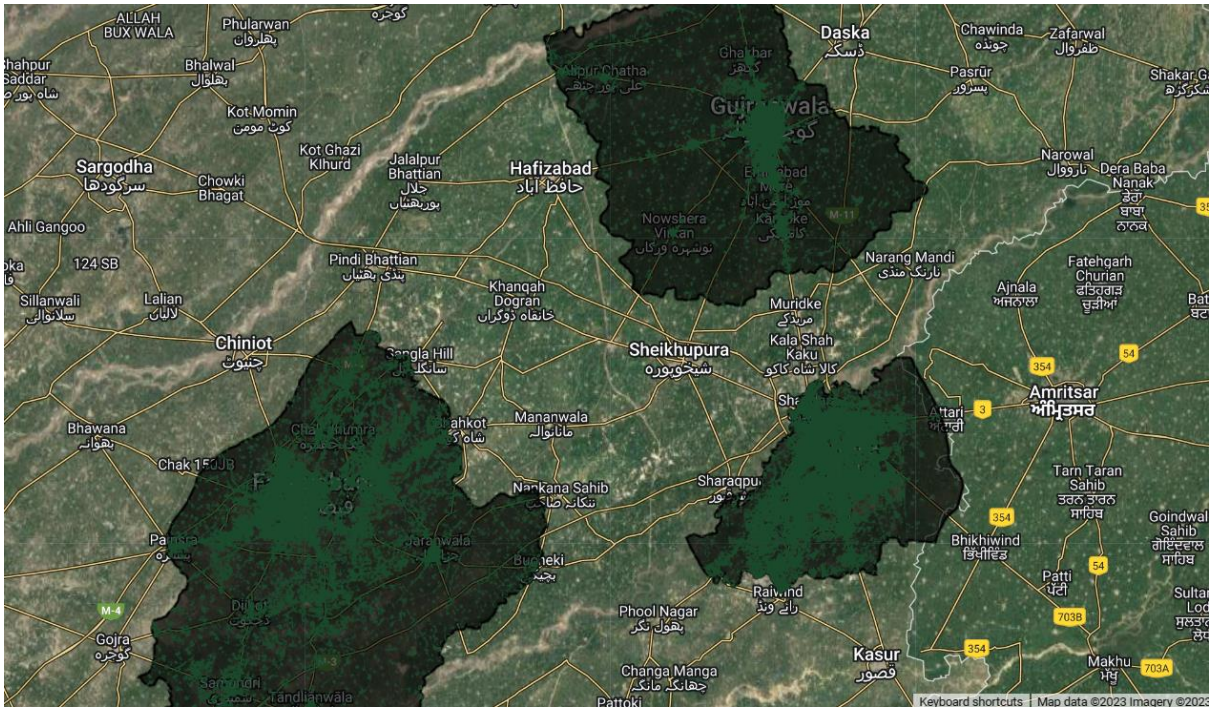

- Increase in Impervious surfaces from 2000 to 2018:

- Overlap of Impervious surface increase from 2000-2018 and floodplain in Lahore district:

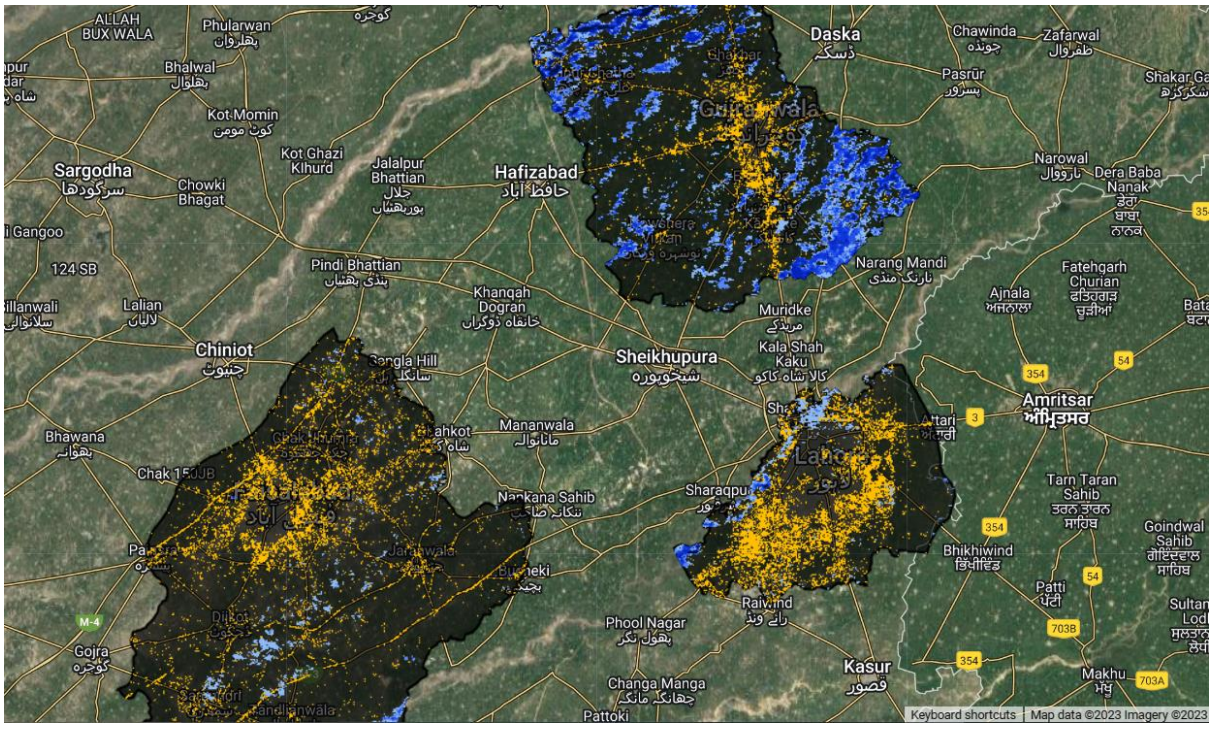

Summary statistics (for Lahore district only):

Area of Impervious Surface 2000	31684.118348142278 hectares
Area of Impervious Surface 2018	47046.77280422048 hectares
Area of Impervious Surface Diff 2000-18	15362.654456078213 hectares
Area of GFD Satellite Observed Flood Plain	16792.00053155991 hectares

C. LAND SURFACE TEMPERATURE

- Five-year (2005-2010) summer composite of daytime land surface temperatures per MODIS sensor on Terra satellite:

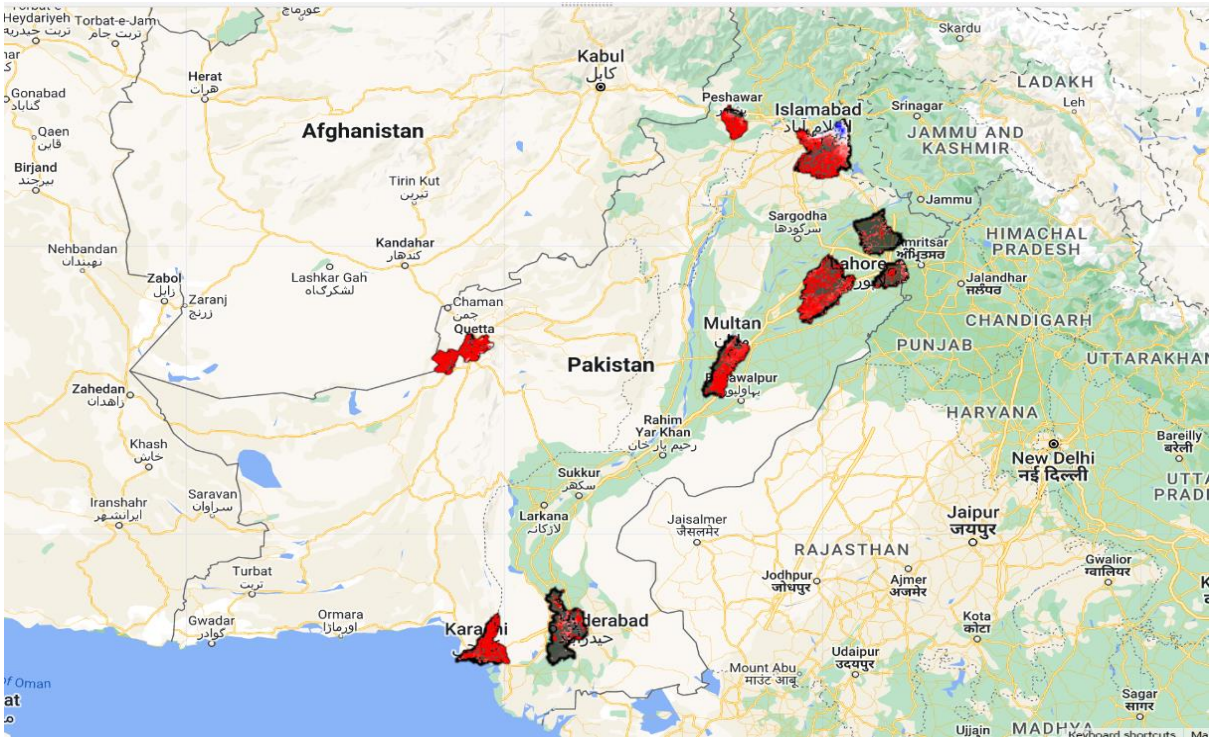

- Five-year (2005-2010) summer composite of daytime land surface temperatures per MODIS sensor on Terra satellite, Lahore district (Average LST for Lahore District: 37.16° C)

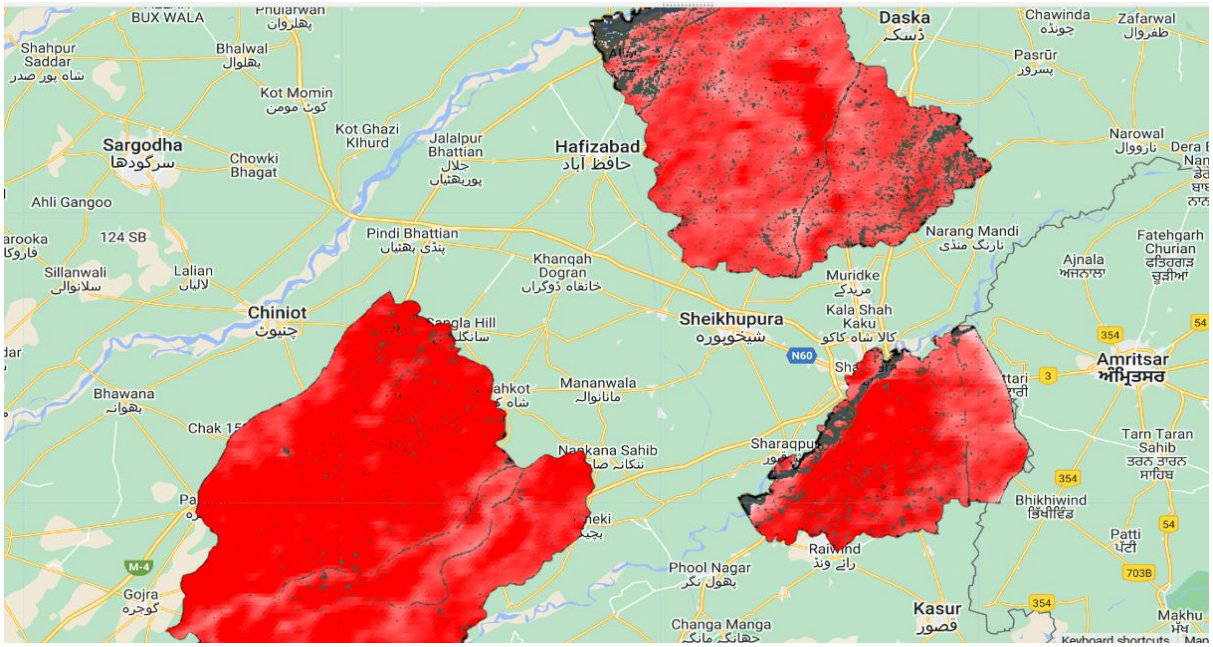

- Five-year (2010-2015) summer composite of daytime land surface temperatures per MODIS sensor on Terra satellite

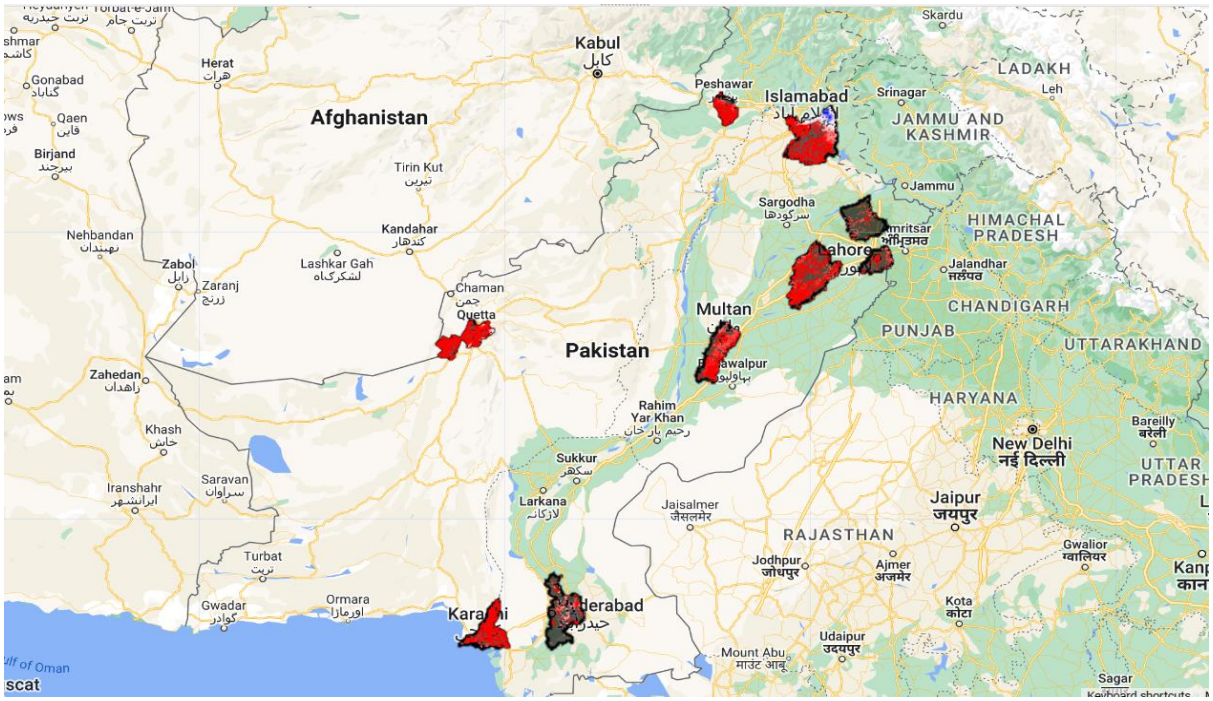

- Five-year (2010-2015) summer composite of daytime land surface temperatures per MODIS sensor on Terra satellite, Lahore district (Average LST for Lahore District: 37.93° C)

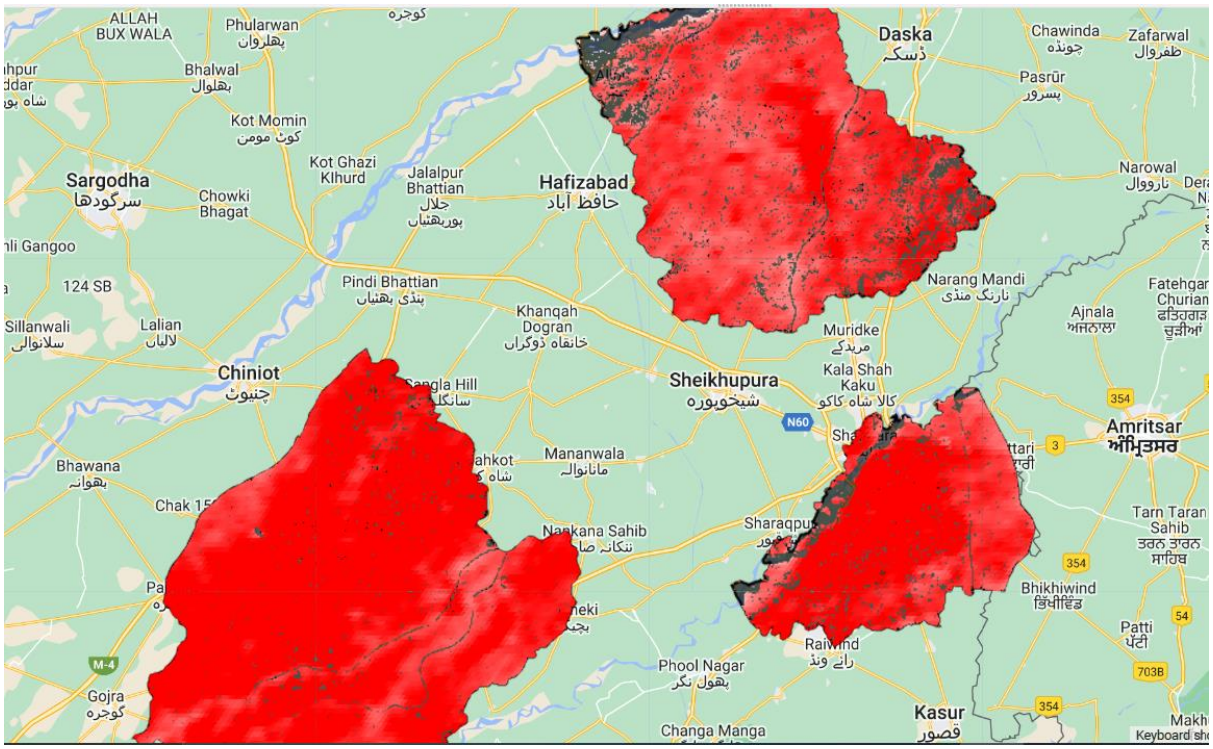

- Five year (2015-2020) summer composite of daytime land surface temperatures per MODIS sensor on Terra satellite

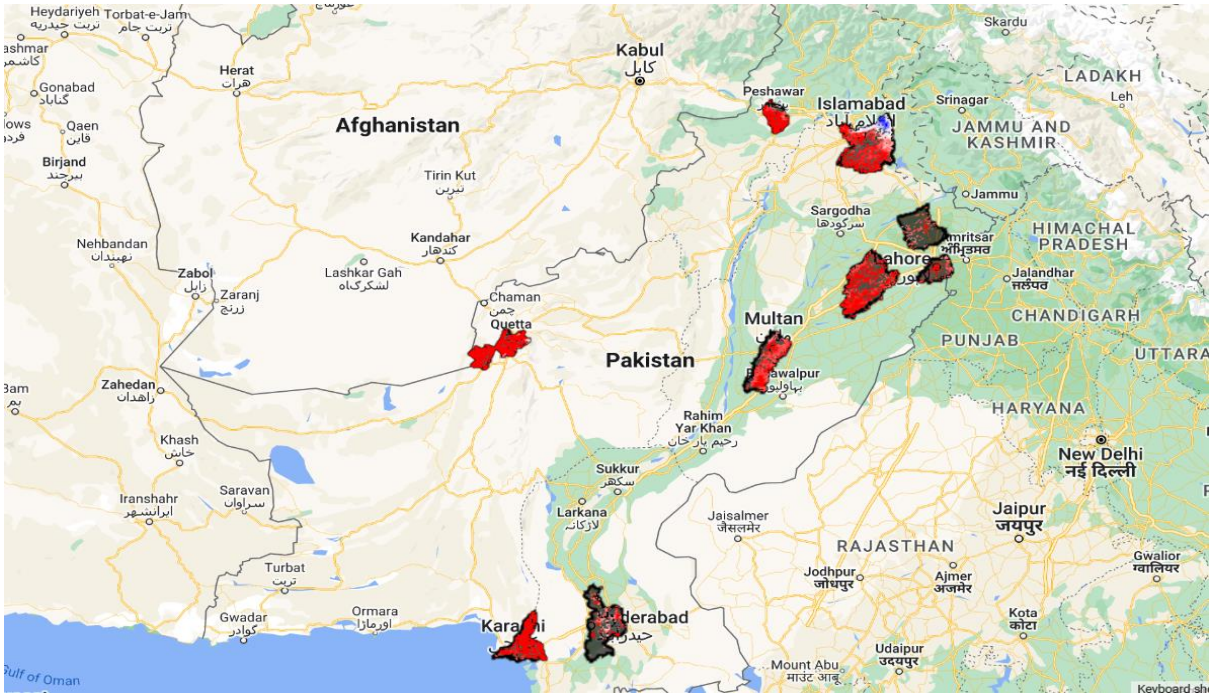

- Five year (2015-2020) summer composite of daytime land surface temperatures per MODIS sensor on Terra satellite, Lahore district (Average LST for Lahore District: 37.37° C)

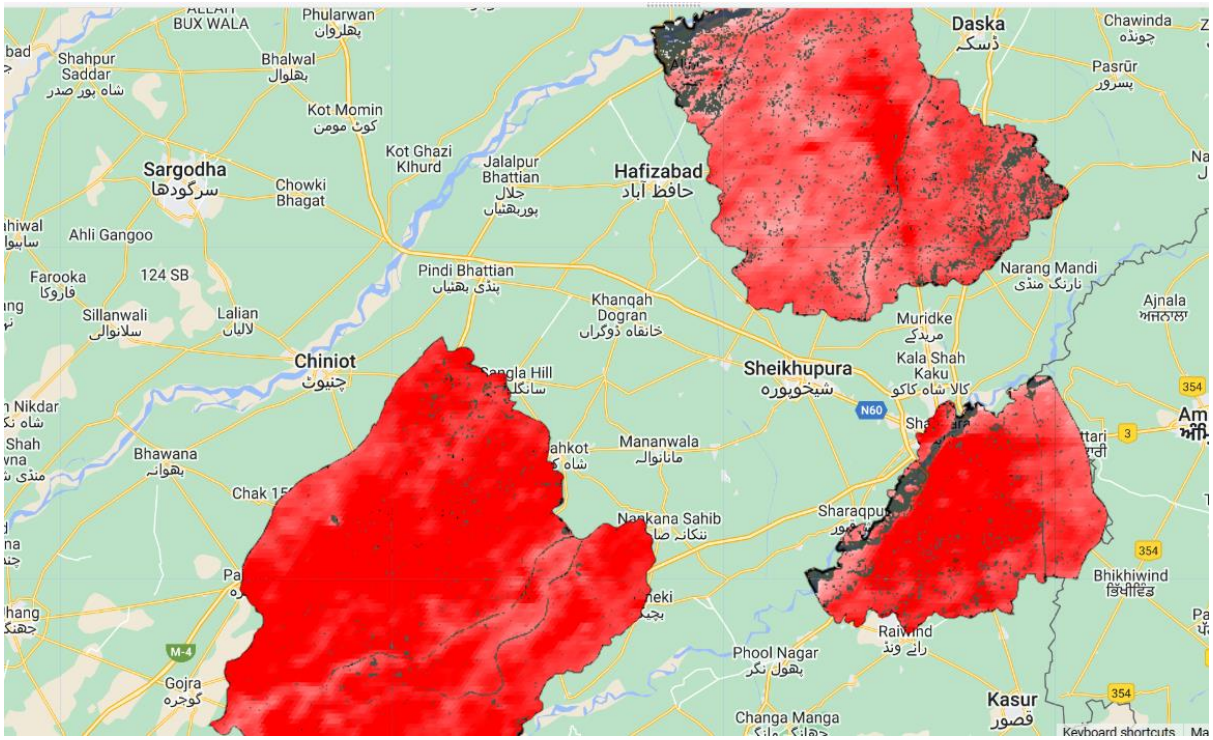

D. COMPARISON OF LAHORE AND LARKANA IN PAKISTAN FLOOD OF 2022

- Lahore district in August 2022:

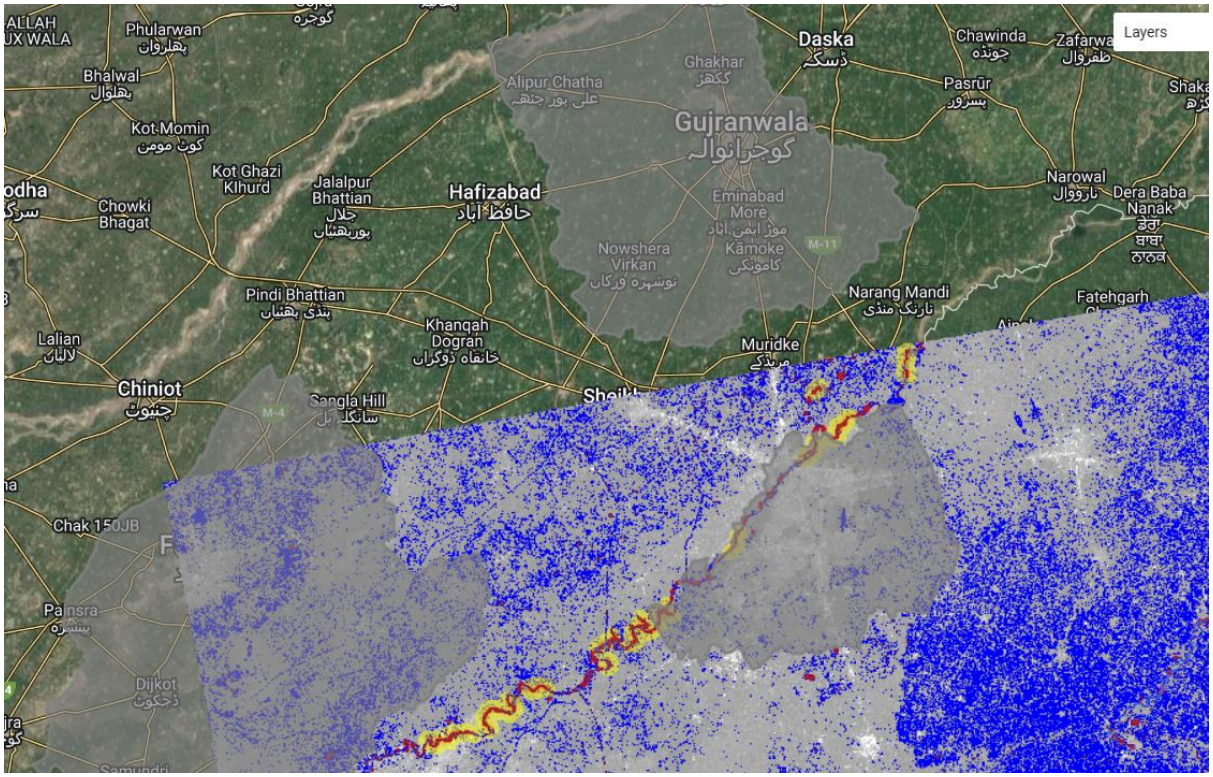

- Larkana, Sindh (affected area on bank of river Indus) in August 2022:

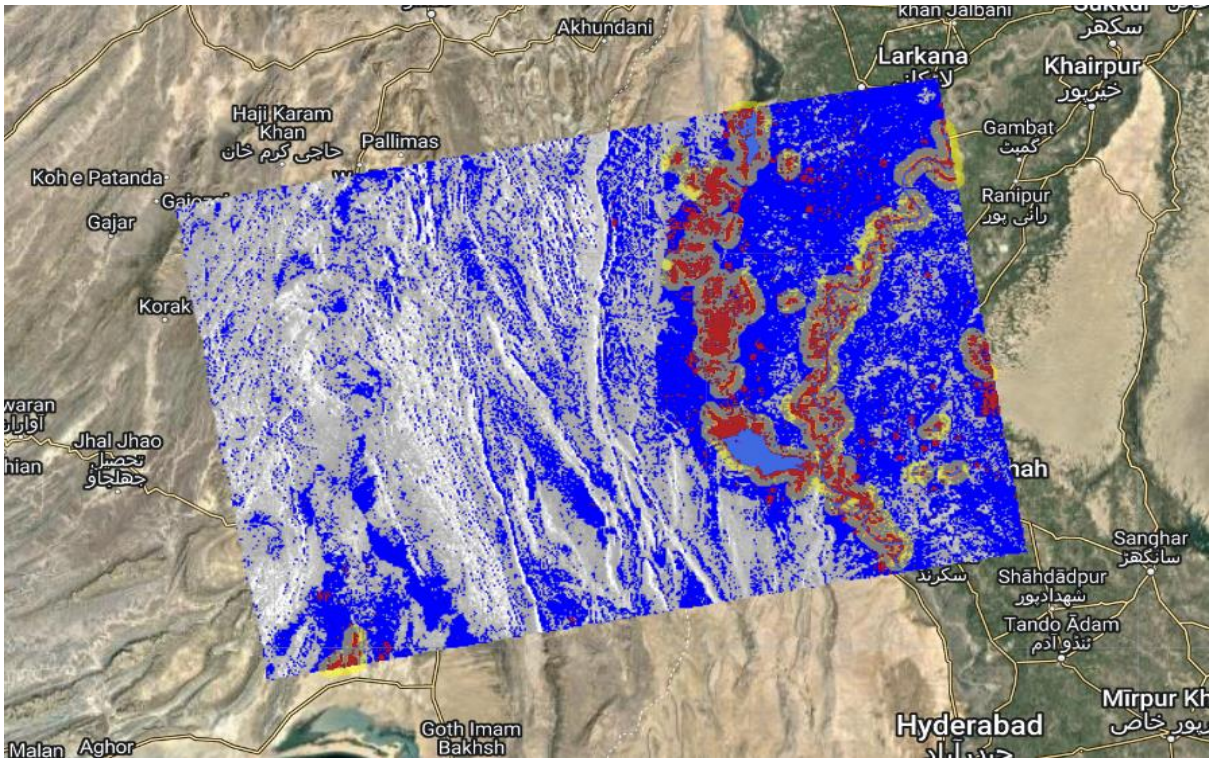

E. WATER BALANCE

- Mean monthly precipitation, Pakistan 2010-2020:

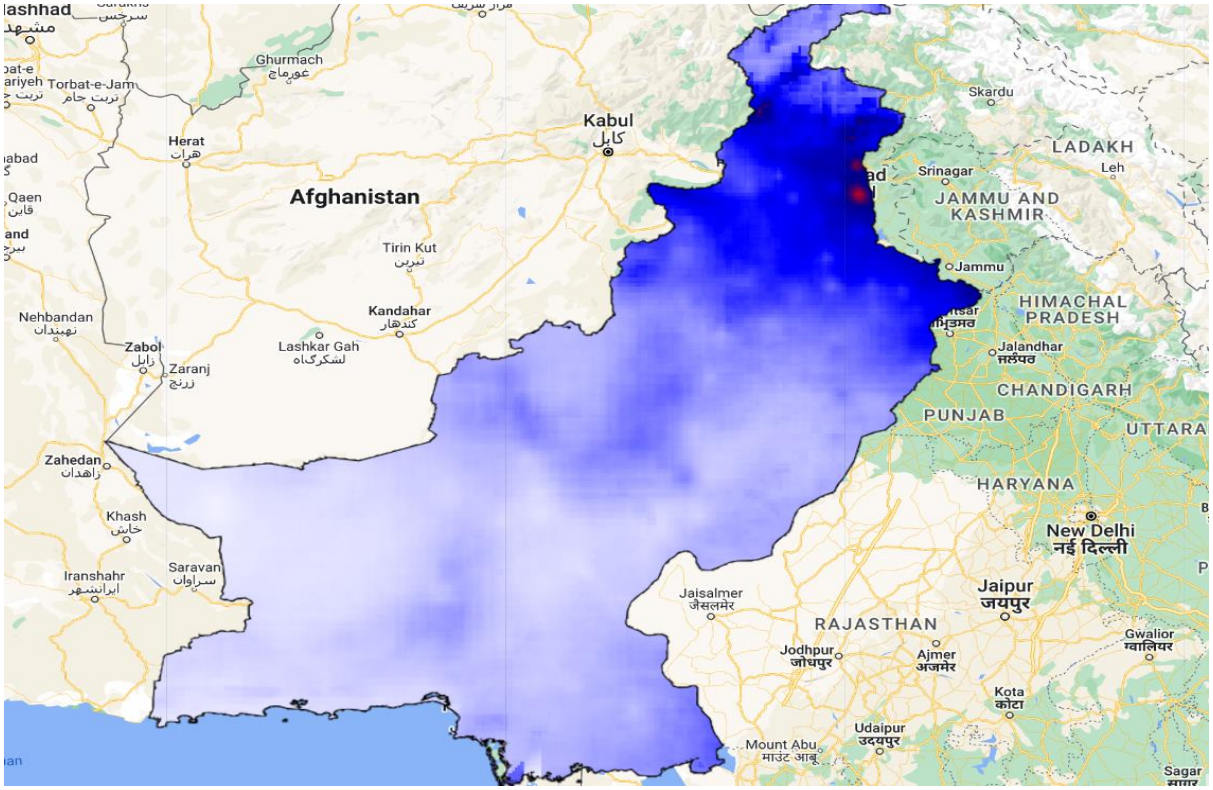

- Mean monthly precipitation, Pakistan 2010 to 2020:

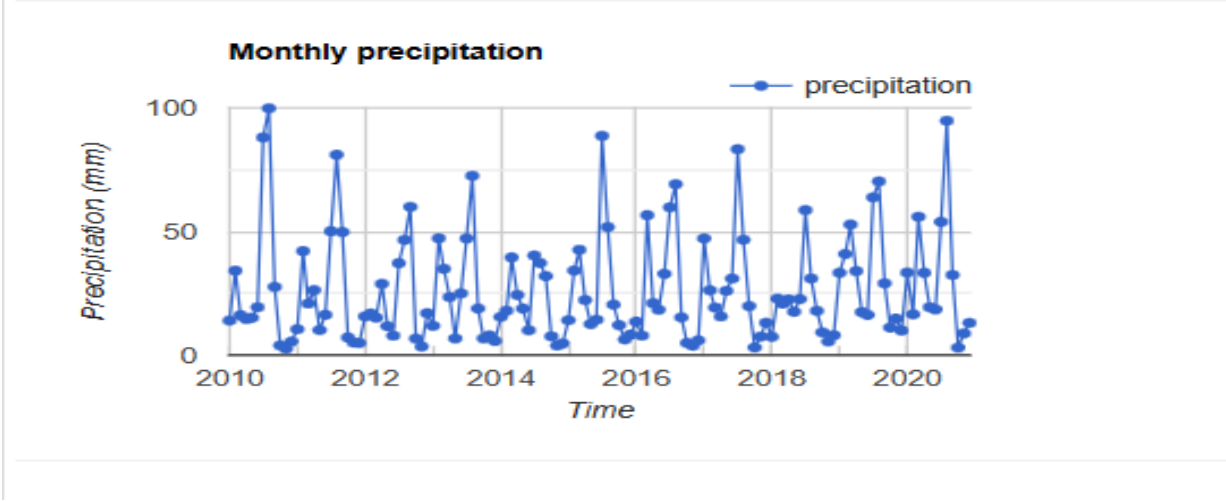

- Mean monthly precipitation, Lahore district 2010-2020:

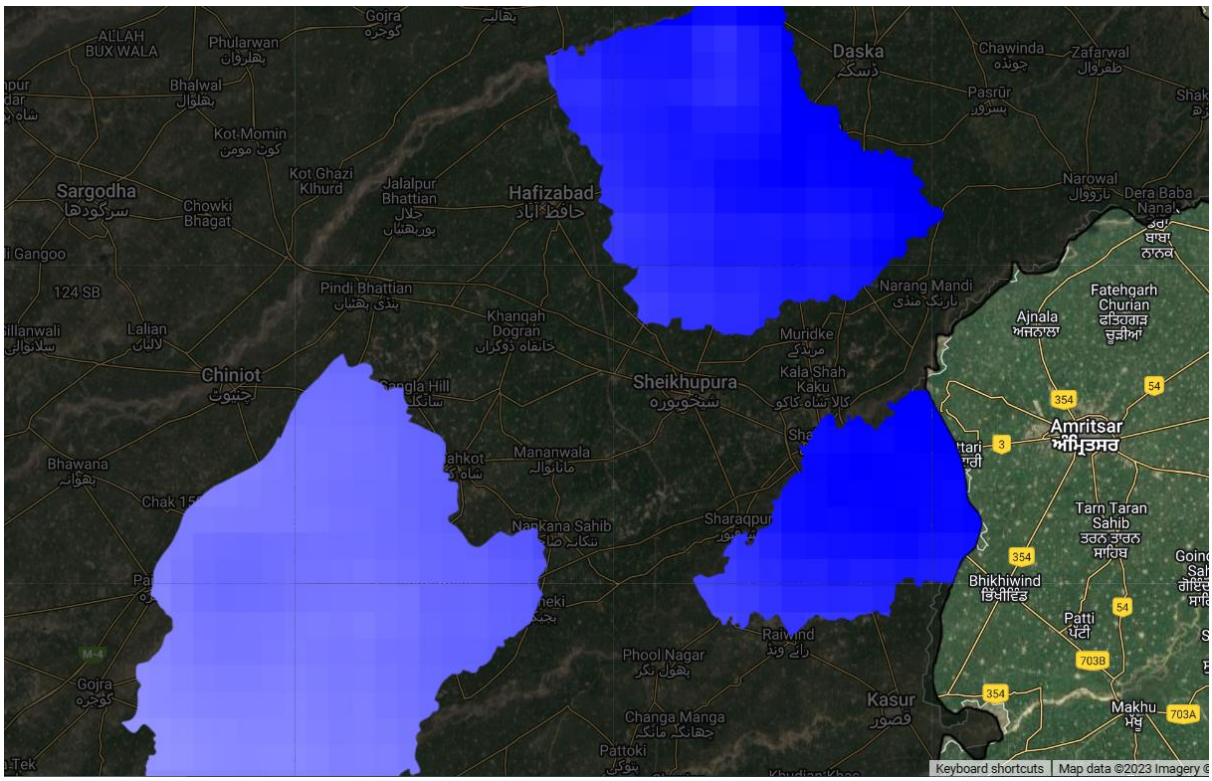

Year	Month	Mean Precipitation
2010	1	9.63
2010	2	20.23
2010	3	15.49
2010	4	5.40
2010	5	15.46
2010	6	19.60
2010	7	203.33
2010	8	204.26
2010	9	97.47
2010	10	4.71
2010	11	2.54
2010	12	8.01
2020	1	48.65
2020	2	14.90
2020	3	79.55
2020	4	28.43
2020	5	23.30
2020	6	53.89
2020	7	201.21
2020	8	295.83
2020	9	76.96
2020	10	2.81
2020	11	9.58
2020	12	18.09

- Mean monthly evapotranspiration, Pakistan 2010-2020:

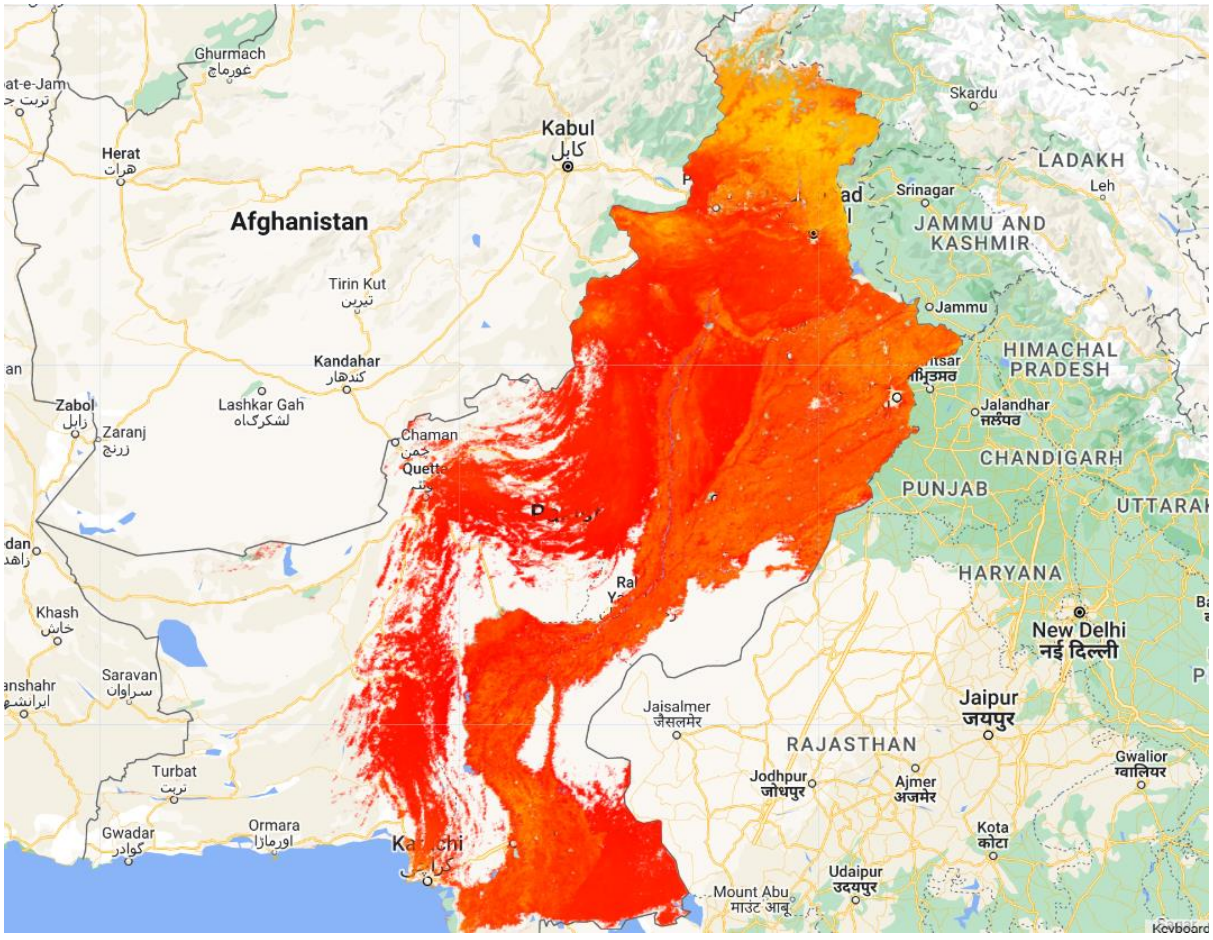

- Mean monthly evapotranspiration, Pakistan 2010 to 2020:

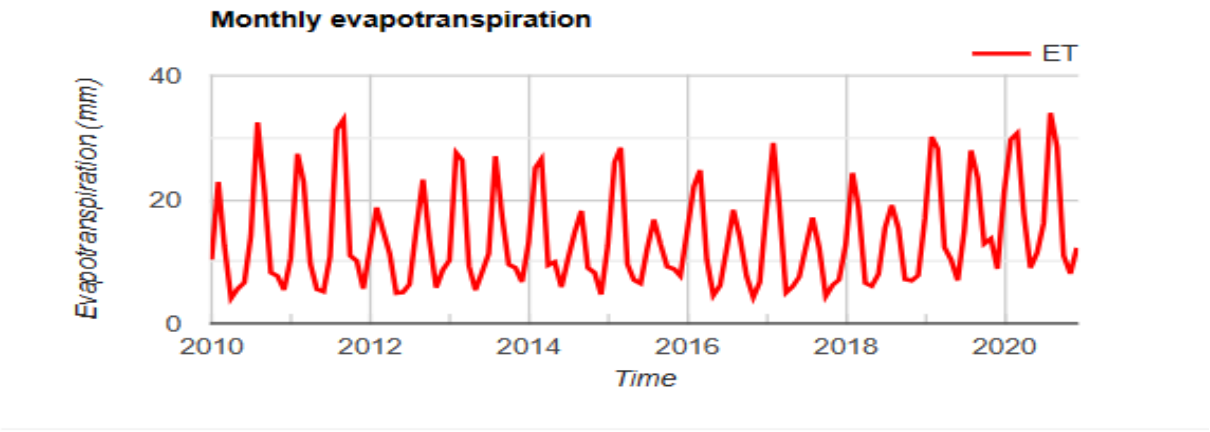

- Mean monthly evapotranspiration, Lahore district 2010-2020:

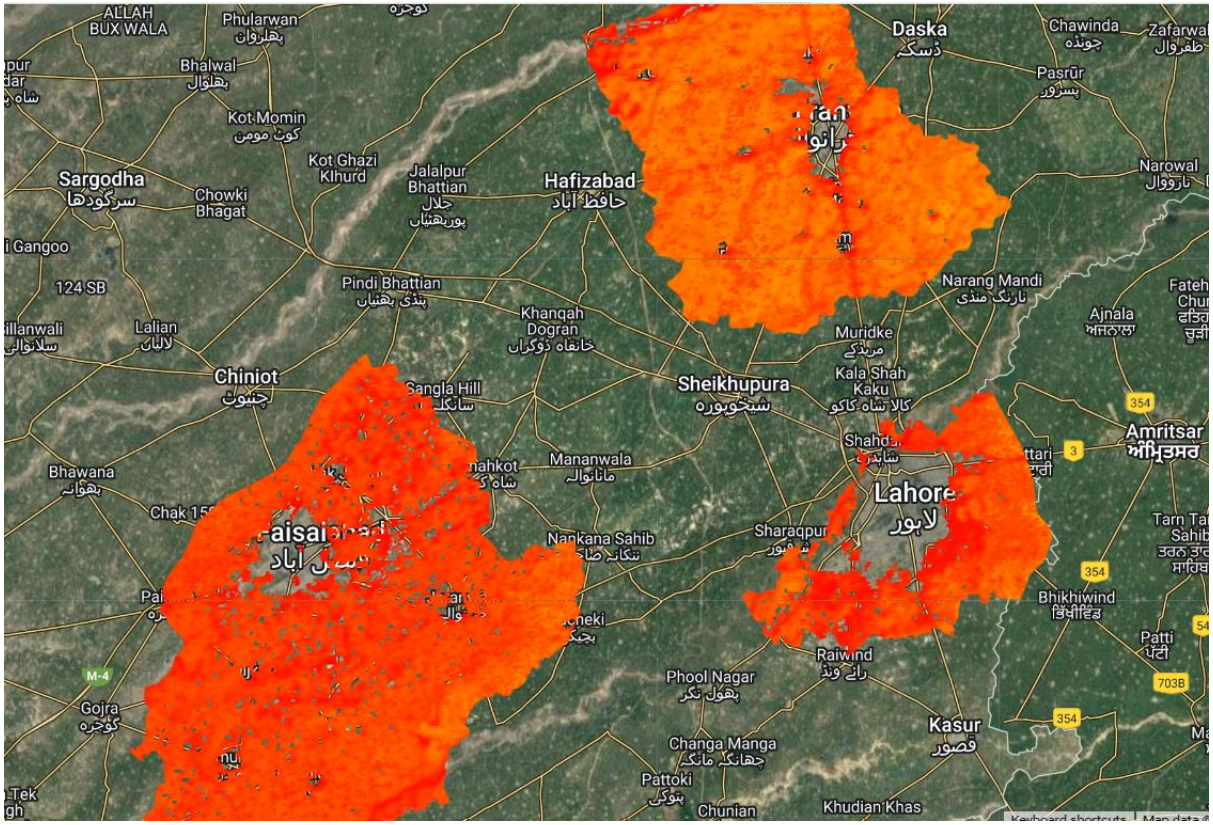

Year	Month	Mean Evapotranspiration			
2010	1	11.53 mm	2020	1	25.59 mm
2010	2	44.94 mm	2020	2	54.15 mm
2010	3	25.45 mm	2020	3	53.57 mm
2010	4	0.67 mm	2020	4	25.84 mm
2010	5	0.39 mm	2020	5	6.14 mm
2010	6	0.33 mm	2020	6	2.39 mm
2010	7	10.48 mm	2020	7	10.47 mm
2010	8	25.35 mm	2020	8	33.16 mm
2010	9	28.15 mm	2020	9	24.97 mm
2010	10	8.11 mm	2020	10	8.33 mm
2010	11	8.98 mm	2020	11	9.26 mm
2010	12	8.77 mm	2020	12	13.76 mm

- Monthly Water Balance, Pakistan 2010-2020:

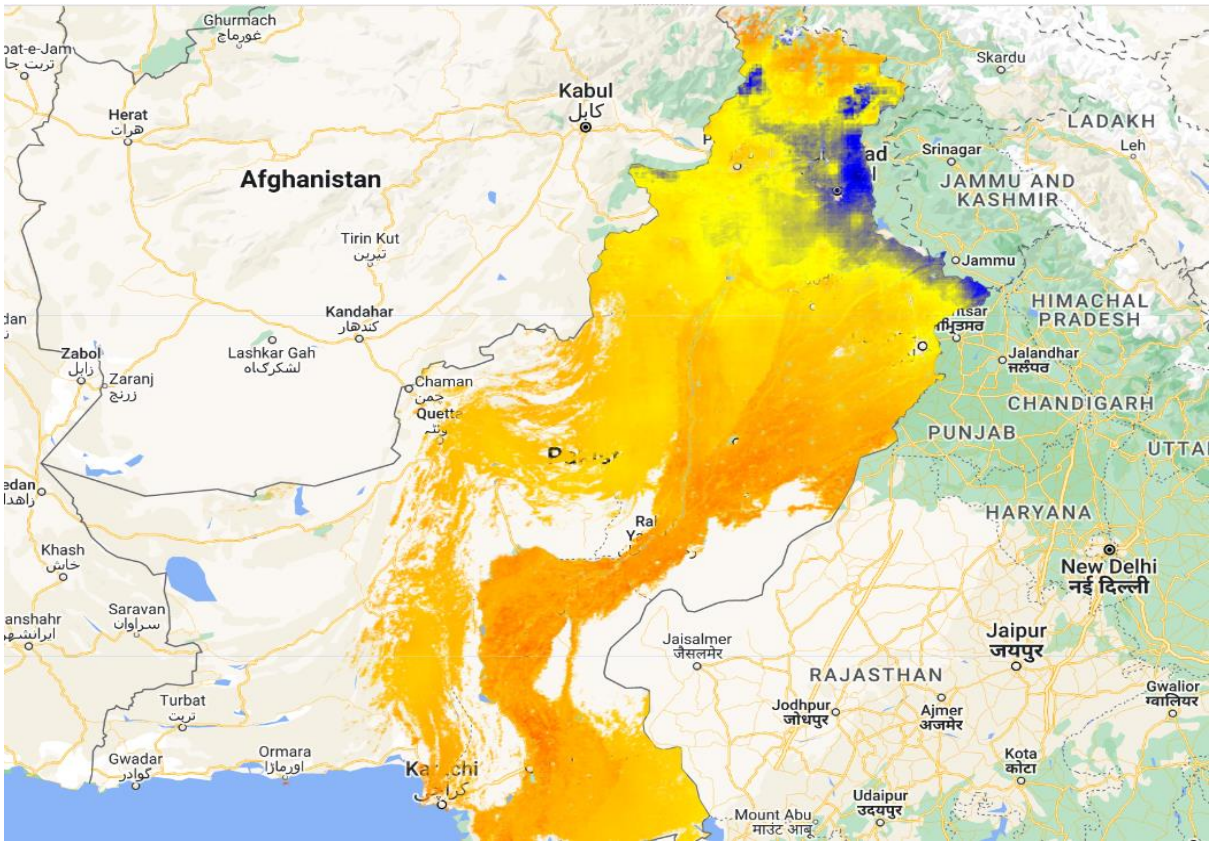

- Monthly Water Balance Lahore, 2010 to 2020:

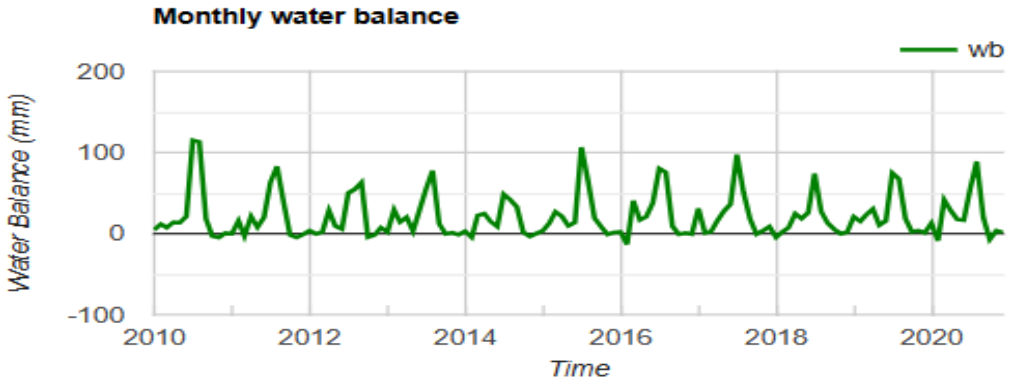

- Monthly Water Balance, Lahore district 2010-2020:

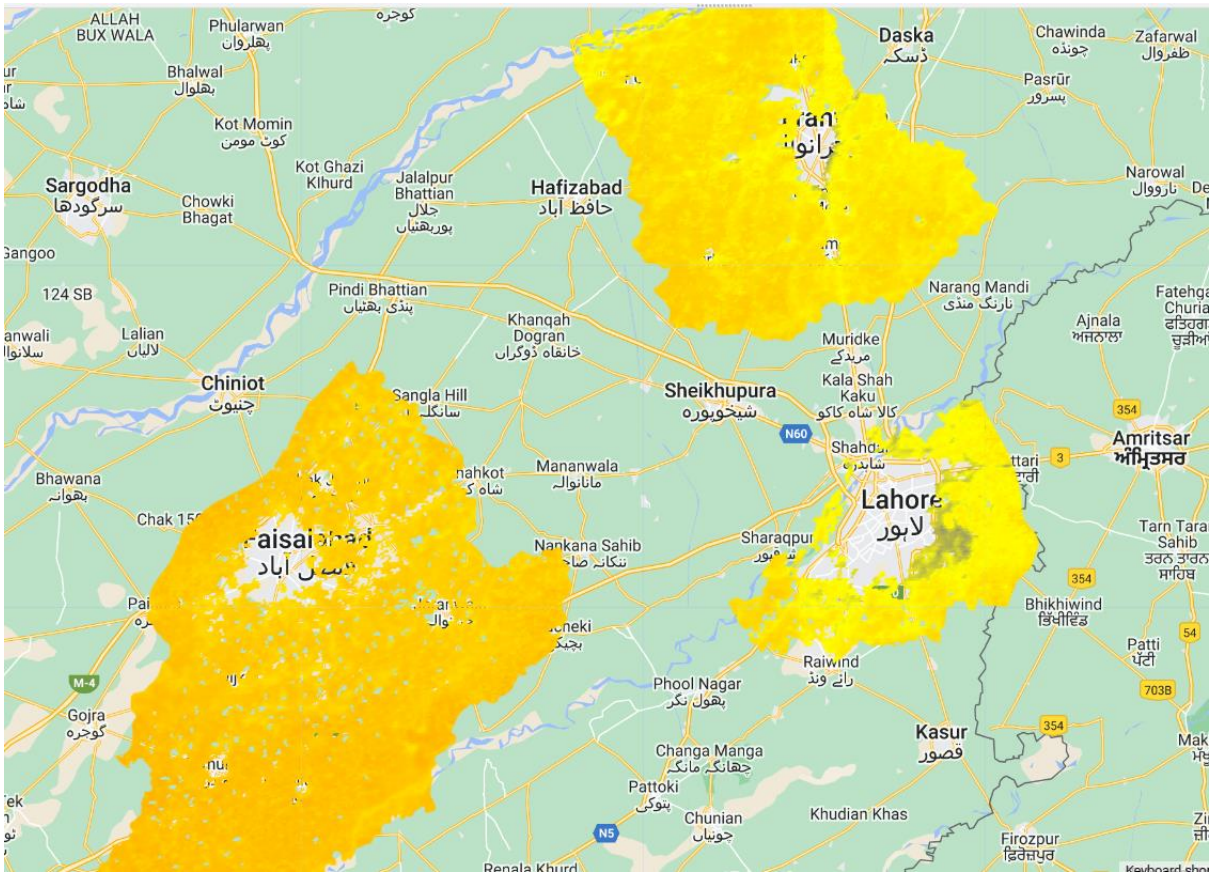

Year	Month	Mean Water Balance	Year	Month	Mean Water Balance
2010	1	-1.73 mm	2020	1	24.42 mm
2010	2	-24.55 mm	2020	2	-38.61 mm
2010	3	-10.05 mm	2020	3	25.06 mm
2010	4	4.61 mm	2020	4	2.60 mm
2010	5	14.29 mm	2020	5	16.25 mm
2010	6	19.59 mm	2020	6	51.57 mm
2010	7	190.11 mm	2020	7	185.98 mm
2010	8	177.40 mm	2020	8	258.14 mm
2010	9	65.87 mm	2020	9	50.42 mm
2010	10	-3.39 mm	2020	10	-5.46 mm
2010	11	-6.37 mm	2020	11	0.63 mm
2010	12	-0.87 mm	2020	12	4.07 mm

- Enhanced Vegetation Index, Pakistan 2010-2020:

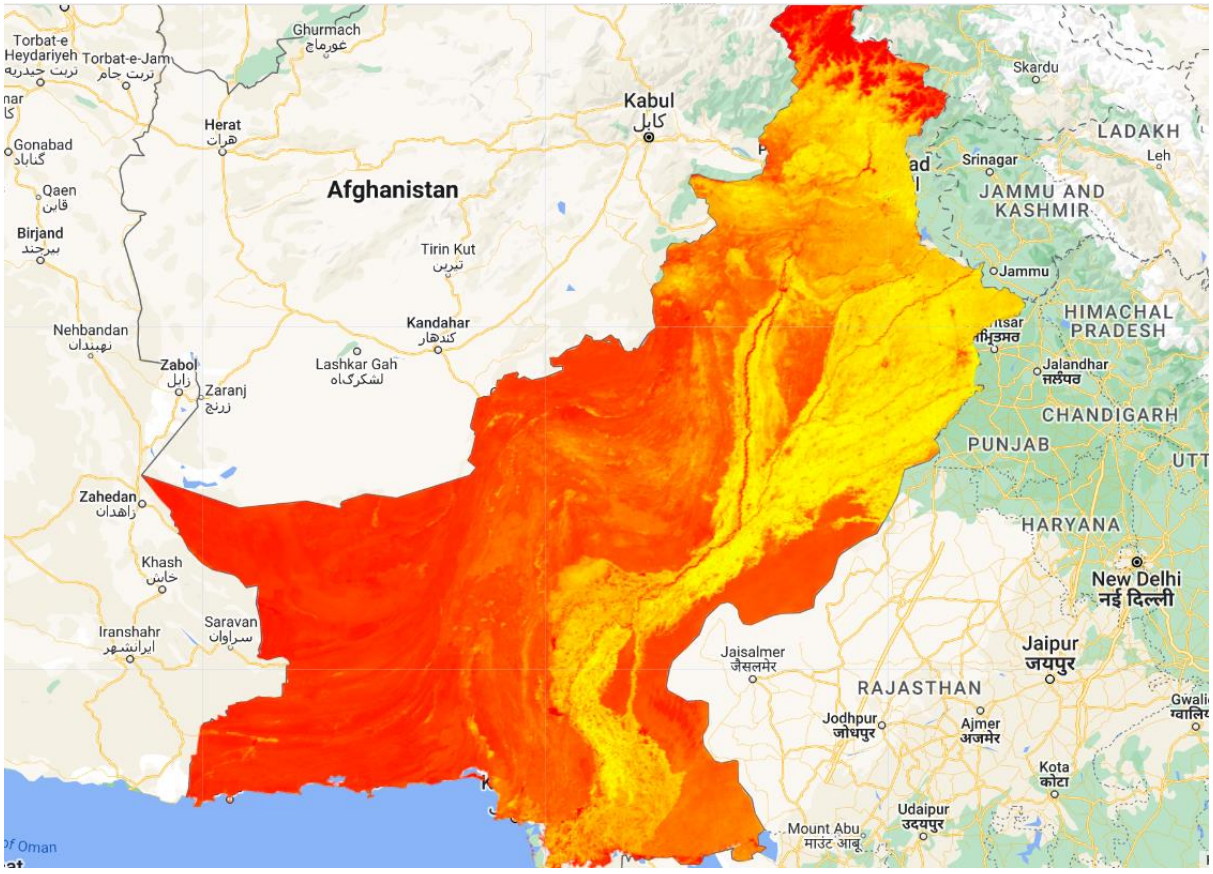

- Enhanced Vegetation Index, Lahore district 2010-2020:

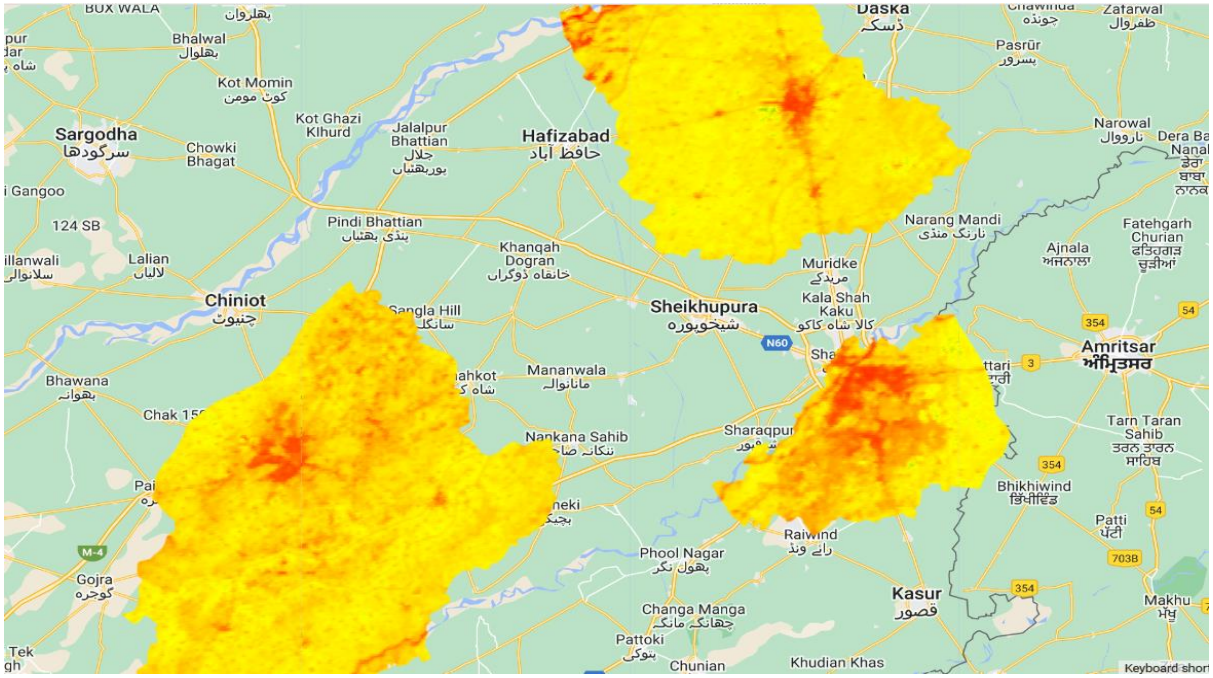

- Moisture Stress Index, Pakistan 2010-2020:

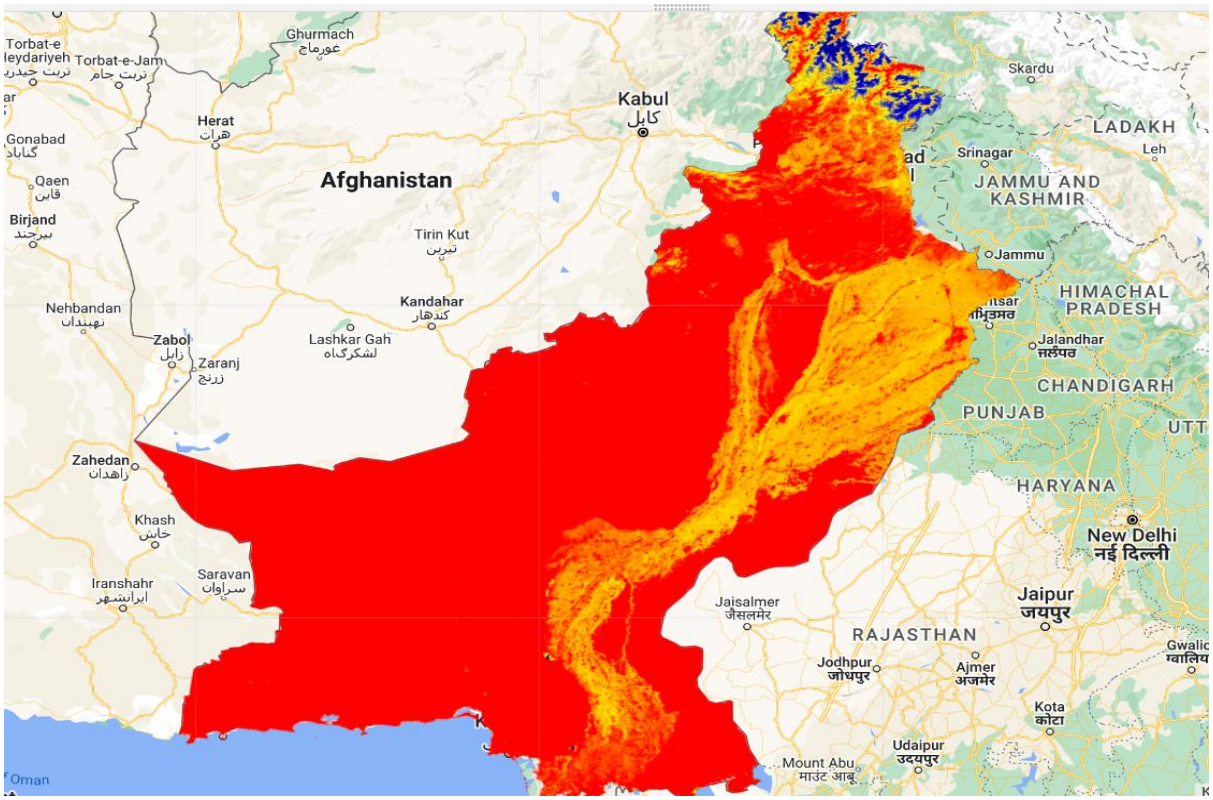

- Moisture Stress Index, Lahore district 2010-2020:

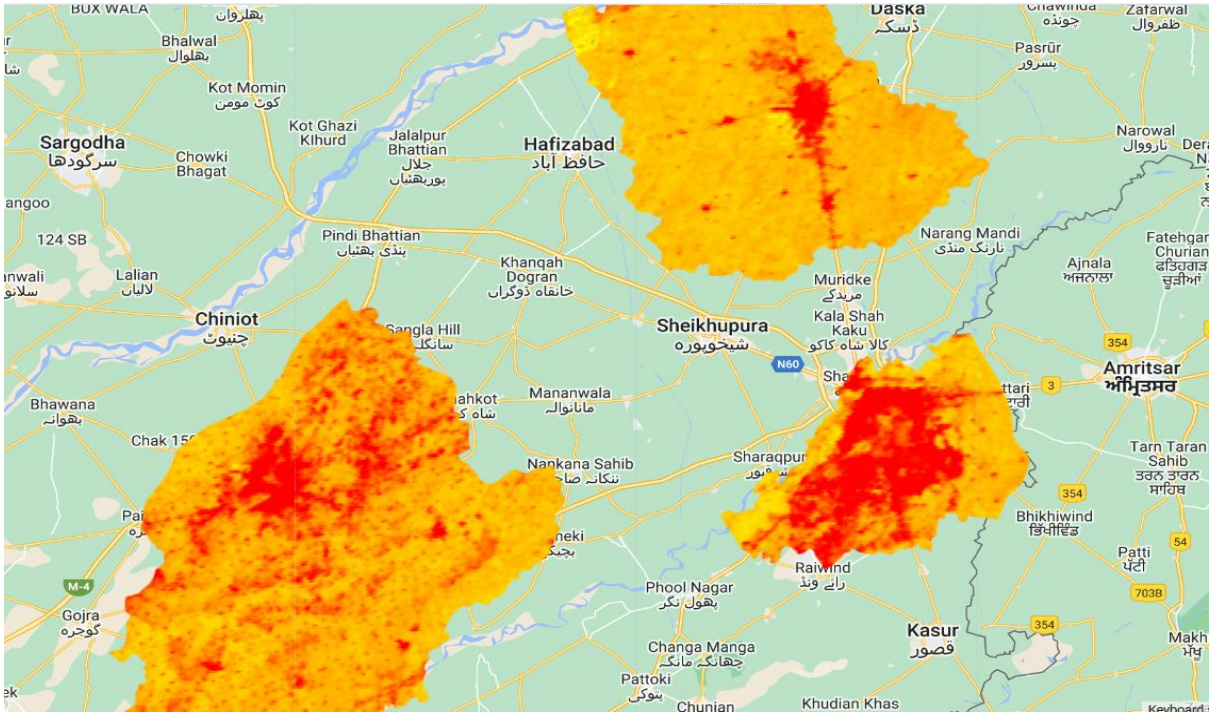

- Mean EVI and MSI, Lahore district 2010 to 2020:

Year	Mean EVI	Year	Mean MSI
2010	0.2309	2010	0.8854
2011	0.2559	2011	0.8526
2012	0.2350	2012	0.8721
2013	0.2572	2013	0.8483
2014	0.2405	2014	0.8527
2015	0.2509	2015	0.8544
2016	0.2398	2016	0.8883
2017	0.2383	2017	0.8915
2018	0.2348	2018	0.8951
2019	0.2641	2019	0.8640
2020	0.2668	2020	0.8475

F. LAND COVER CHANGE

- Rangeland cover: World Cover 2020 palette:

Serial No.	Land Cover Type	Color
0	Tree cover	Dark Green
1	Shrubland	Vivid Orange
2	Grassland	Canary Yellow
3	Cropland	Light Magenta
4	Built-up	Red
5	Bare/sparse vegetation	Light Gray
6	Snow and ice	Very Light Gray
7	Permanent water bodies	Strong Blue
8	Herbaceous wetland	Teal
9	Mangroves	Medium Green
10	Moss and lichen	Light Cream

- World Cover 2020 Lahore district:

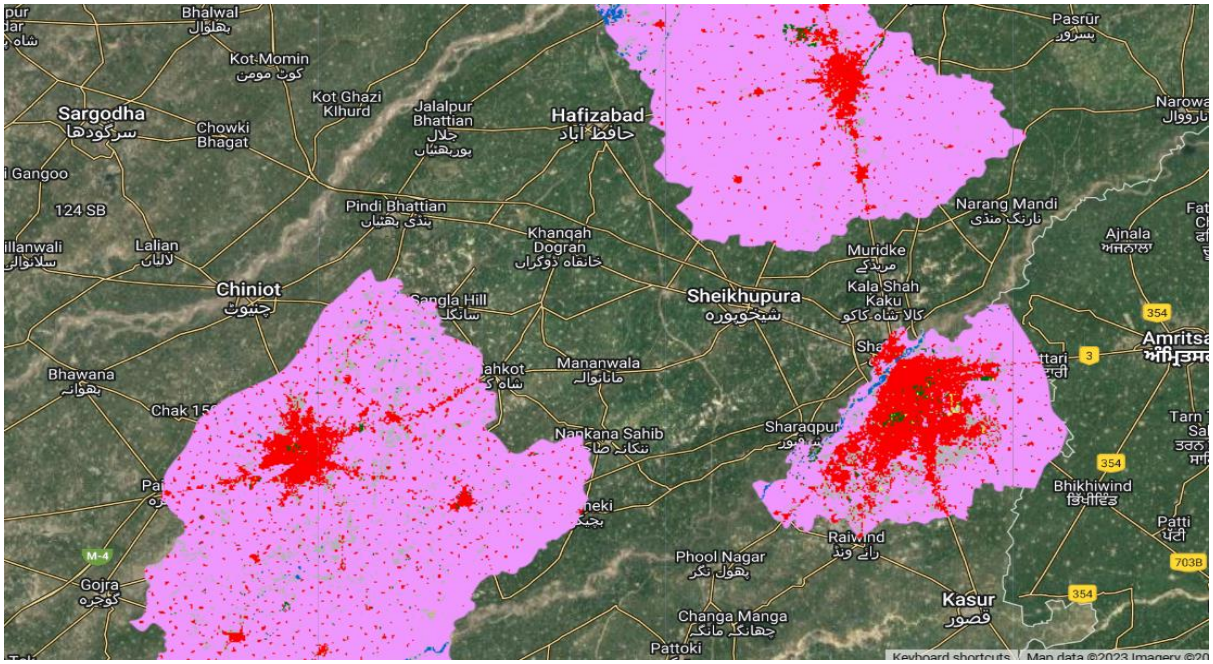

© ESA WorldCover project / Contains modified Copernicus Sentinel data (2020) processed by ESA WorldCover consortium

- Modis 2001 Pakistan:

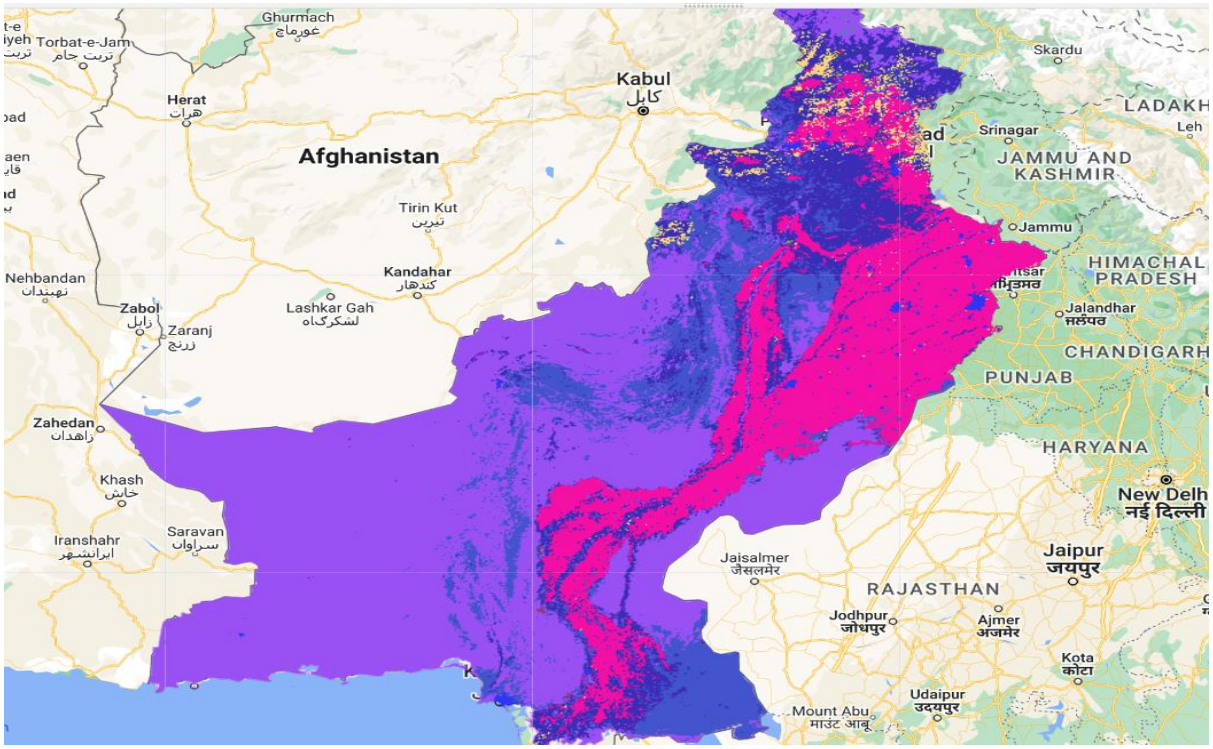

- Modis 2001 Lahore district:

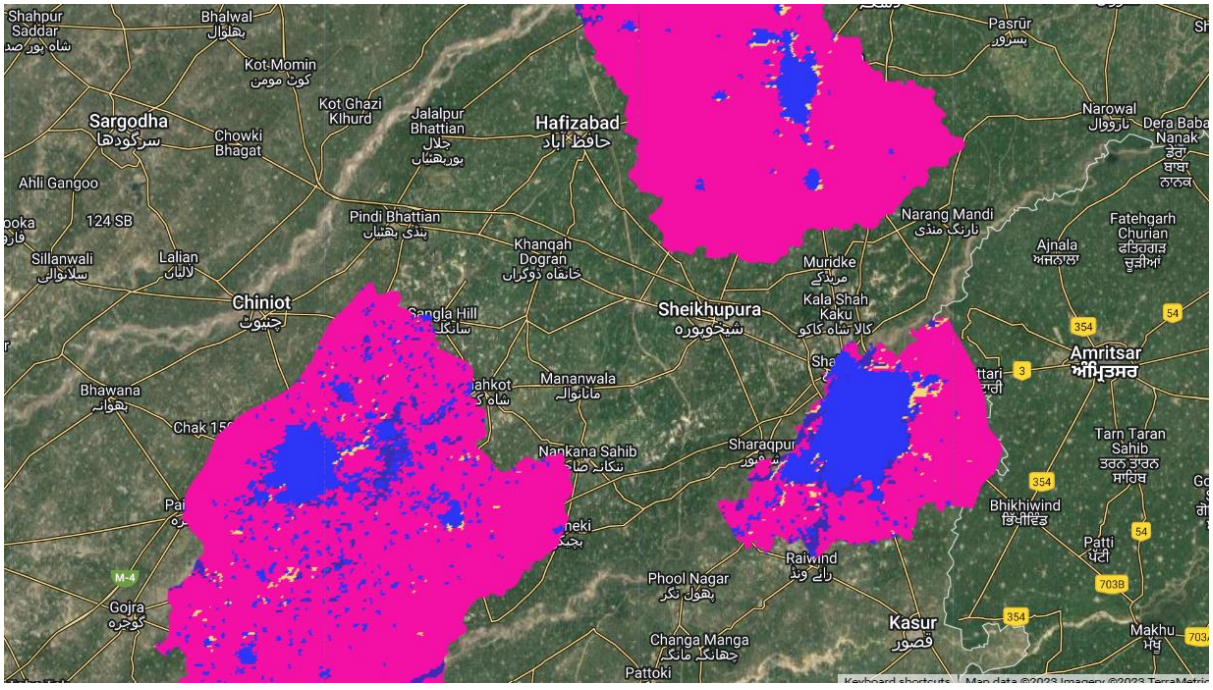

- Modis 2016 Pakistan:

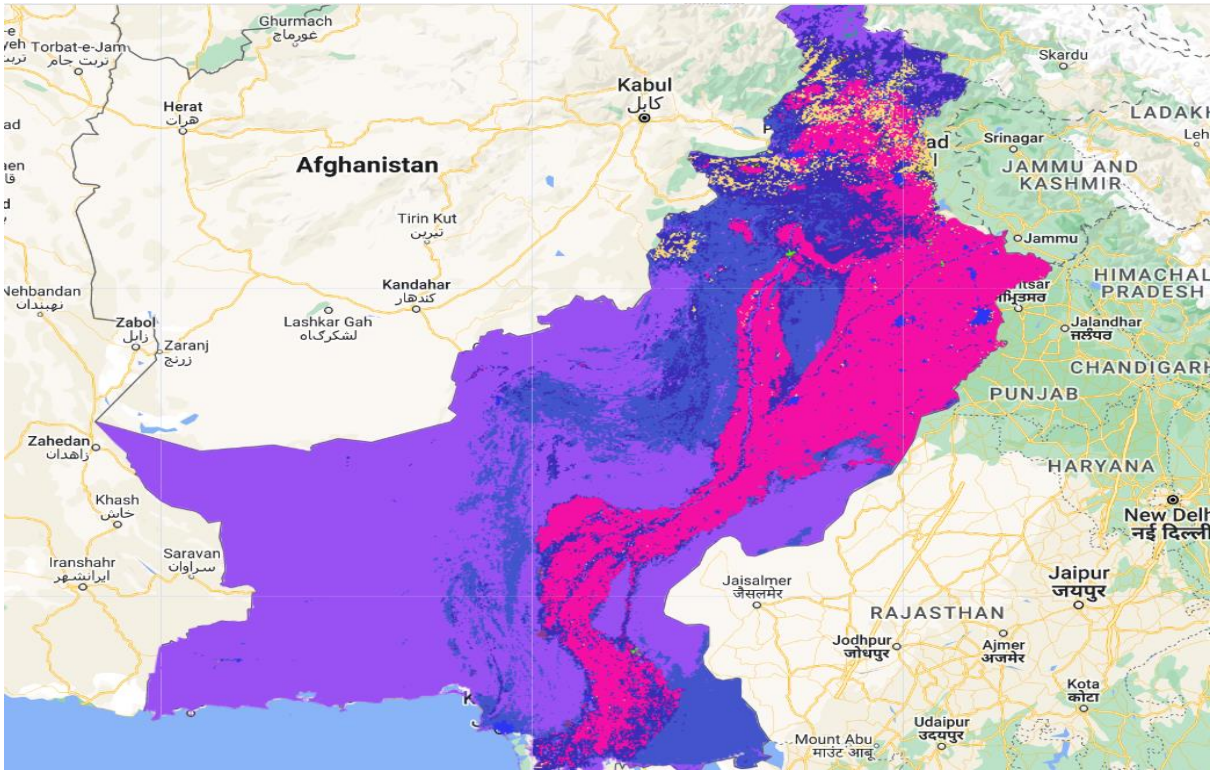

- Modis 2016 Lahore district:

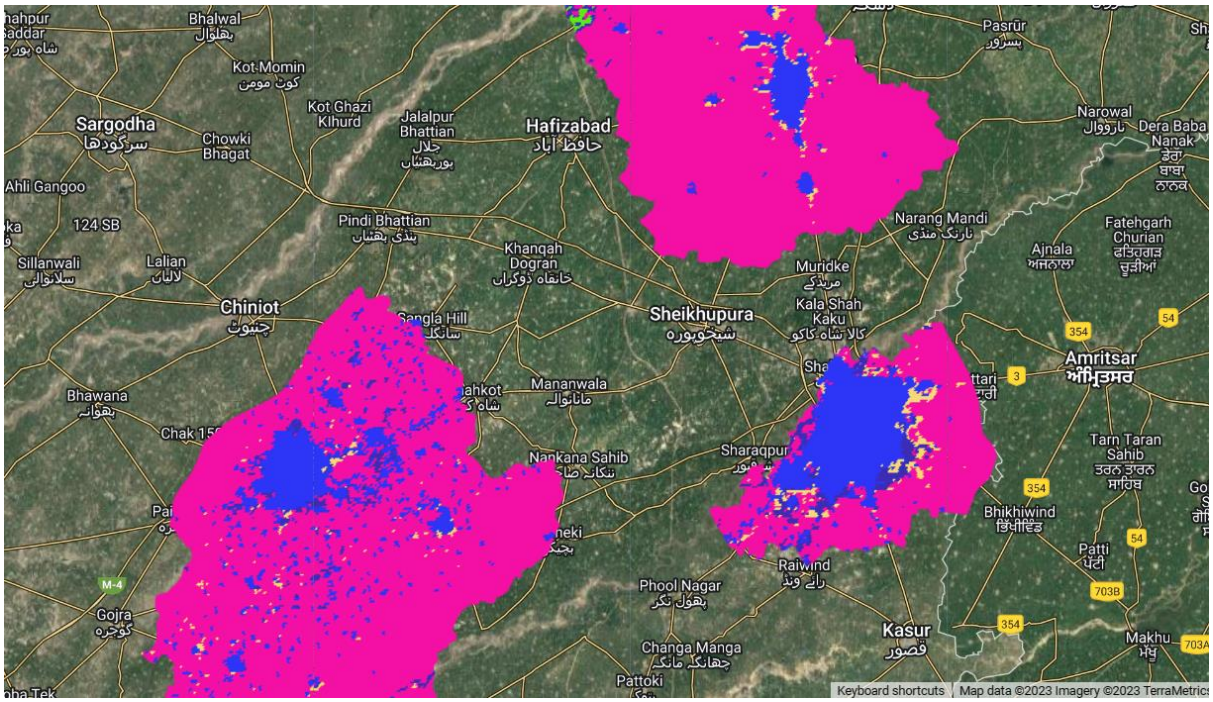

Band 12: Croplands: at least 60% of area is cultivated cropland

Dataset	Band (12)
Land Cover Areas for 2001	1,049,381,611.2906 sq. m
Land Cover Areas for 2009	1,026,948,360.2576 sq. m
Land Cover Areas for 2016	968,995,604.4340 sq. m

III. Interpretation

a. Population Expanse

Visually, a comparison of the WorldPop dataset for 2000 and 2020 demonstrates visible population growth between 2000 and 2020 towards the south and east of the Lahore district boundaries along the arteries connecting Lahore city with its adjoining districts. An increase in the concentration of population in already inhabited areas is also demonstrated by the brighter population footprint visible in the 2020 image. The population estimates calculated using the Global Human Settlement Layer are 4,970,158 for the year 1990, 6,449,726 for the year 2000 and 8,923,281 for the year 2015. These figures equal a 2.98% per year population growth rate in the Lahore district from 1990 to 2000 and a 2.56% population growth rate from 2000 to 2015, which are both high figures.

b. Urban Expansion and Floodplain

Visually, the floodplain in Lahore district is a continuation of the River Ravi flowing in across the border through India from the north east, and the total impervious surface cover seems to overlap with the floodplain area. When a separate layer of impervious surface growth in Lahore from 2000 to 2018 is superimposed on the floodplain area, a 6.92 square kilometer area is found, indicating that in this 18 year period, 6.92 square kilometers of floodplain has been covered by impervious surfaces.

c. Land Surface Temperature

Land Surface Temperature may be increased by the growth of urban structures which changes the amount of radiation absorbed and reflected by new surfaces. This increase may also be reinforced by the clearing of vegetation to make way for urban expansion as it reduces the cooling effect of evapotranspiration from vegetation. Changes in surface properties can alter local climate (Kalnay and Cai 2003) and give rise to phenomena such as the Urban Heat Island effect (Arnfield 2003; Qian et al 2022).

The composite daytime land surface temperature in Lahore district from 2005 to 2010 is 37.16 degrees Celsius; from 2010 to 2015 is 37.93 degrees Celsius and from 2015 to 2020 is 37.37 degrees Celsius. A comparison of these three averages shows that at the five year level during this period, there does not appear to be an increasing or decreasing trend in the land surface temperatures in the Lahore district. However it is possible that annual estimates may demonstrate an increasing or decreasing trend.

d. Water Balance

In the water balance equation, precipitation is equal to the sum of runoff, evapotranspiration and changes in groundwater and soil storage. The monthly mean precipitation in this study is derived from the CHIRPS dataset. MOD16 is used for the estimation of evapotranspiration. The Enhanced Vegetation Index from MODIS is used as the vegetation index. The Moisture Stress Index (calculated from the shortwave infrared and near infrared bands) is calculated as an indicator of soil moisture. All these variables indicate either a surplus of water, or water stress, shedding light on the general tendency towards drought-like conditions in the region of interest. In Lahore, generally the water balance appears to be consistent overall, with the balance chart showing apparently regular oscillations through the seasons in the period under examination.

e. Rangeland Cover

Based on the WorldCover 2020 dataset, most of the Lahore district area is comprised of either built up area or cropland. When cropland area for 2001, 2009 and 2016 is estimated using the concerned MODIS dataset, a clearly declining trend becomes visible: the annual percentage change in cropland is -0.27% from 2001 to 2009, and -0.81% from 2009 to 2016. This indicates that area used agriculturally in the Lahore district is declining faster with time.

f. Synthesis

While population growth in the Lahore district remains high, cropland is actually decreasing. Although further analysis of the food requirements of Lahore's population would be required to estimate how significant the decline in cropland is, generally in a country which has a similar overall population growth rate, a decrease in agricultural area in the absence of agri-tech or food security planning may be a warning indicator. The increase in urbanization of the Ravi floodplain from 2000 to 2018 is also a warning indicator for adaptation considering the increasing unpredictability and extent of monsoon floods in Pakistan. Based on the estimation of water balance and land surface temperature indicators in Lahore in this study, there does not appear to be an overall warming or drought intensifying trend.

IV. Conclusion

The goal of this study was to determine, based on trends derived from geo-spatial data, whether urbanization and demographic trends in Pakistan's Lahore district are generally in harmony with the requirement for climate adaptive development. While in this research there is no indication of increasing water scarcity or rise in temperatures in the area of interest over the 20-odd year period studied, the intrusion of urban surfaces into floodplain areas and the decline in agricultural area may indicate that policymakers need to reign in these particular trends, which may otherwise increase the vulnerability of the population to climate disasters. Researchers may also need to focus particularly on the impact of climate change on food security in Pakistan for more specific data regarding trends and the requirements for self-sufficiency. Similarly, a more in-depth analysis of each water balance indicator estimated in this study may help isolate trends towards water scarcity that are not visible in a macro analysis. Regression analyses of the various indicators may help credibly establish the correlation between interconnected facets of the human and climate ecosystem in Pakistan, enabling policymakers to have a systems view of the evolving situation.

Considering the non-parallel trajectories of climate at local and global levels, a theory of change may be needed which can resolve these local and regional differences, while also accounting for the interactions between the human and the climate which give rise to very complex networks of agency. Such an approach may be the way to address the compound climate risk that arises from the interaction of human and ecological systems, both locally and globally.

REFERENCES

Nanditha, J. S., et al. "The Pakistan flood of August 2022: Causes and implications." Earth's Future 11.3 (2023): e2022EF003230.

Reuters, Sophia Saifi, Akanksha Sharma and Asim Khan for CNN, and. “33 Million People Hit by Pakistan Floods, Minister Says.” CNN, 26 Aug. 2022, www.cnn.com/2022/08/25/asia/pakistan-flooding-climate-minister-intl-hnk/index.html.

“See the Scale of Pakistan’s Flooding in Maps, Photos and Videos.” Washington Post, 31 Aug. 2022, www.washingtonpost.com/world/2022/08/31/pakistan-floods-photos-videos-maps/.

“Devastating Floods in Pakistan.” NASA, NASA, earthobservatory.nasa.gov/images/150279/devastating-floods-in-pakistan. Accessed 21 Aug. 2023.

Two years in the Life of the Indus River Basin." (2013). In Winston Yu, Yi-Chen Yang, Andre Savitsky, Donald Alford, Casey Brown, James Wescoat, Dario Debowicz, and Sherman Robinson. “The Indus Basin of Pakistan” (April 18, 2013). p.17-33.

“Population Growth (Annual %) - Pakistan.” World Bank Open Data, data.worldbank.org/indicator/SP.POP.GROW?locations=PK. Accessed 21 Aug. 2023.

Arslan, Muhammad. “Housing Projects Killing Farmland: Heinrich-Böll-Stiftung Afghanistan/Pakistan.” Heinrich-Böll-Stiftung, 18 Aug. 2022, afpak.boell.org/en/2022/08/18/housing-projects-killing-farmland.

WorldPop (www.worldpop.org - School of Geography and Environmental Science, University of Southampton; Department of Geography and Geosciences, University of Louisville; Departement de Geographie, Universite de Namur) and Center for International Earth Science Information Network (CIESIN), Columbia University (2018). Global High Resolution Population Denominators Project - Funded by The Bill and Melinda Gates Foundation (OPP1134076). https://dx.doi.org/10.5258/SOTON/WP00645

Schiavina M., Freire S., Carioli A., MacManus K. (2023): GHS-POP R2023A - GHS population grid multitemporal (1975-2030).European Commission, Joint Research Centre (JRC) PID: http://data.europa.eu/89h/2ff68a52-5b5b-4a22-8f40-c41da8332cfe, doi:10.2905/2FF68A52-5B5B-4A22-8F40-C41DA8332CFE

Xin Huang, Jiayi Li, Jie Yang, Zhen Zhang, Dongrui Li, & Xiaoping Liu. (2021). 30 m global impervious surface area dynamics and urban expansion pattern observed by Landsat satellites: from 1972 to 2019 (Version 1.0.0) [Data set]. http://doi.org/10.1007/s11430-020-9797-9

Tellman, B., J.A. Sullivan, C. Kuhn, A.J. Kettner, C.S. Doyle, G.R. Brakenridge, T. Erickson, D.A. Slayback. (Accepted.) Satellites observe increasing proportion of population exposed to floods. Nature. doi:10.1038/s41586-021-03695-w

Copernicus Sentinel data 2022, processed by ESA.

Running, S., Mu, Q., Zhao, M. (2021). MODIS/Terra Net Evapotranspiration 8-Day L4 Global 500m SIN Grid V061 [Data set]. NASA EOSDIS Land Processes Distributed Active Archive Center. Accessed 2023-08-21 from https://doi.org/10.5067/MODIS/MOD16A2.061

Didan, K. (2021). MODIS/Terra Vegetation Indices 16-Day L3 Global 250m SIN Grid V061 [Data set]. NASA EOSDIS Land Processes Distributed Active Archive Center. Accessed 2023-08-21 from https://doi.org/10.5067/MODIS/MOD13Q1.061

Friedl, M., Sulla-Menashe, D. (2022). MODIS/Terra+Aqua Land Cover Type Yearly L3 Global 500m SIN Grid V061 [Data set]. NASA EOSDIS Land Processes Distributed Active Archive Center. Accessed 2023-08-21 from https://doi.org/10.5067/MODIS/MCD12Q1.061

Zanaga, D., Van De Kerchove, R., De Keersmaecker, W., Souverijns, N., Brockmann, C., Quast, R., Wevers, J., Grosu, A., Paccini, A., Vergnaud, S., Cartus, O., Santoro, M., Fritz, S., Georgieva, I., Lesiv, M., Carter, S., Herold, M., Li, Linlin, Tsendbazar, N.E., Ramoino, F., Arino, O., 2021. ESA WorldCover 10 m 2020 v100. https://doi.org/10.5281/zenodo.5571936

Jean-Francois Pekel, Andrew Cottam, Noel Gorelick, Alan S. Belward, High-resolution mapping of global surface water and its long-term changes. Nature 540, 418-422 (2016). (doi:10.1038/nature20584)